Cloud microphysical relationships and their implication on entrainment and mixing processes in stratocumulus clouds

Seong Soo Yum

Department of Atmospheric Sciences

Yonsei University

In collaboration with

Jian Wang, Yangang Liu, Chunsong Lu, Jae Min Yeom,…

International Workshop on Cloud Dynamics, Microphysics and Small Scale Simulation

August 13-17, 2018

Introduction

- Warm rain initiation problem has been known for several decades but solution to this problem is not completely resolved.
- Among several potential solution to this problem is "entrainment and mixing" that leads to the growth of so called "superadiabatic" droplets.
- In this study we examine cloud microphysical relationships of the clouds measured during several aircraft measurement campaigns to find the implication of such relationships on entrainment and mixing process.
- Does entrainment and mixing promote droplet growth? Maybe not!

Condensational droplet growth equation

$$r\frac{dr}{dt} = \frac{S-1}{\left[\left(\frac{L}{R_v T} - 1\right)\frac{L\varrho_L}{KT} + \frac{\varrho_L R_v T}{De_s(T)}\right]} \equiv \frac{S-1}{[F_k + F_d]}$$

Rogers and Yau (1989)

When solute and curvature effects are included,

$$r\frac{dr}{dt} = \frac{(S-1) - \frac{a}{r} + \frac{b}{r^3}}{[F_k + F_d]}$$

can only be solved numerically!!

F_k and F_d depend on T and p: L, K and e_s(T) are dominantly dependent on T but D is dependent on both T and p.

The condensational growth parameter ξ_1 can be defined:

$$\xi_1 = \frac{1}{F_k + F_d}.$$

For the same S, droplet growth is faster at higher T and lower p (equivalently higher z).

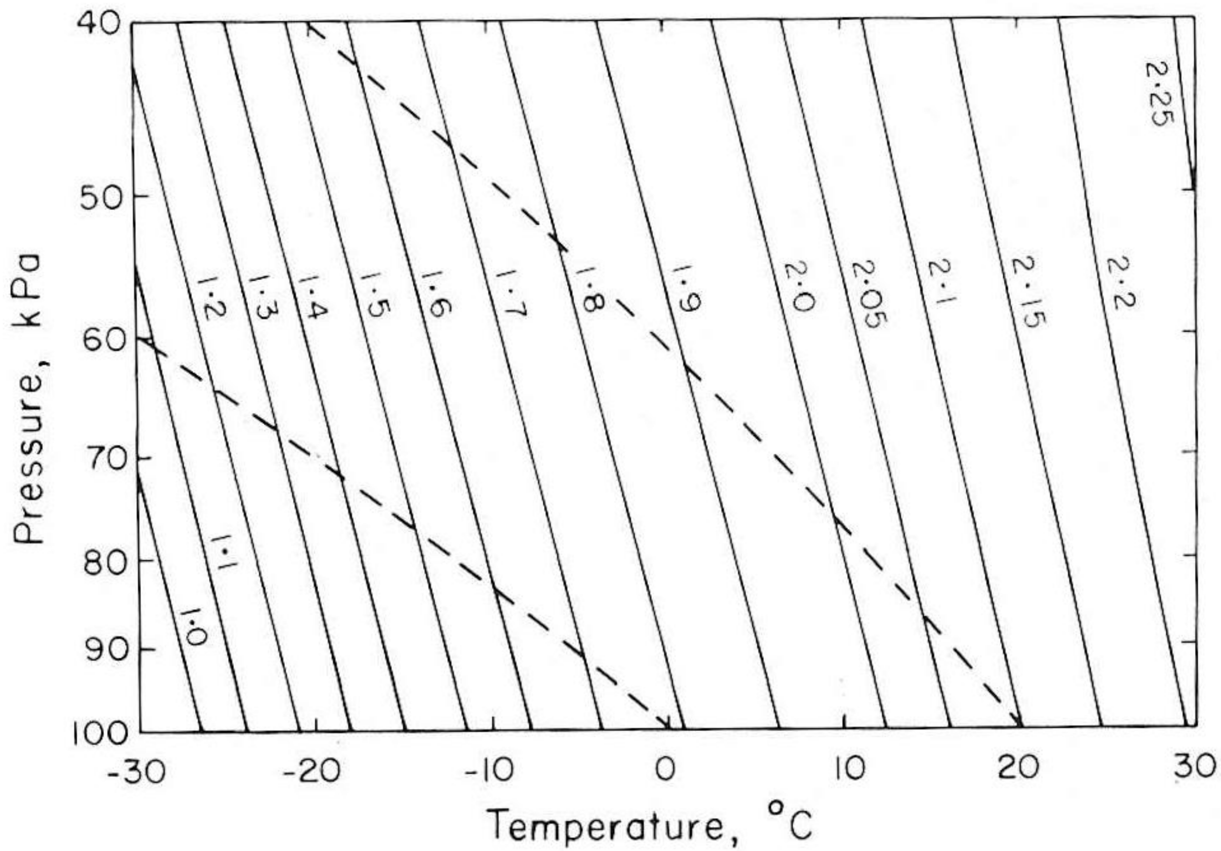

FIG. 7.1. Dependence of the growth parameter $\xi_1 = 1/[F_k + F_d]$ on temperature and pressure. Contours are plotted of the quantity $\log_{10} \xi_1$, with ξ_1 expressed in units of $\mu m^2/s$. Dashed lines represent pseudoadiabats corresponding to $\theta_w = 0°C$ and 20°C.

Rogers and Yau (1989)

S - 1 = 0.05%
p = 90 kPa
T = 273 K
Nucleus: NaCl

TABLE 7.2. *Rate of Growth of Droplets by Condensation (initial radius 0.75 μm). (From Mason, 1971)*

Nuclear mass (g)	10^{-14}	10^{-13}	10^{-12}
Radius (μm)	Time (sec) to grow from initial radius 0.75 μm		
1	2.4	0.15	0.013
2	130	7.0	0.61
4	1,000	320	62
10	2,700	1,800	870
20	8,500	7,400	5,900
30	17,500	16,000	14,500
50	44,500	43,500	41,500

Rogers and Yau (1989)

When r is sufficiently large, neglect solute and curvature terms. Then,

$$r\frac{dr}{dt} \sim \xi, \text{ where } \xi = (S - 1)/[F_k + F_d].$$

Two very important aspects of condensational droplet growth:

$$r(t) = \sqrt{r_0^2 + 2\xi t},$$

$$r_2(t) - r_1(t) = \frac{r_2^2(0) - r_1^2(0)}{r_2(t) + r_1(t)},$$

Rogers and Yau (1989)

-The growth of droplet populations

Droplets interact with their environment and with each other ➔ affect the droplet sizes and concentrations

Saturation ratio controls the growth of droplet population.

$$\frac{dS}{dt} = P - C = Q_1 \frac{dz}{dt} - Q_2 \frac{d\chi}{dt},$$

χ: **Liquid water mixing ratio**

Increase of S due to cooling in adiabatic ascent

Decrease of S due to condensational loss of vapor

$$Q_1 = \frac{1}{T}\left[\frac{\varepsilon L g}{R' c_p T} - \frac{g}{R'}\right]$$

$$Q_2 = \varrho\left[\frac{R'T}{\varepsilon e_s} + \frac{\varepsilon L^2}{p T c_p}\right].$$

Rogers and Yau (1989)

P: can be derived with the assumption that no loss of moisture by condensation during ascent. That is, water vapor mixing ratio does not vary.

C: can be calculated with similar assumption (i.e., condensation but no ascent)

U = 15 cm s^{-1}, CCN of NaCl with moderate conc. (initial T is not given)

$$\frac{dS}{dt} = P - C$$

$$r\frac{dr}{dt} = \frac{(S-1) - \frac{a}{r} + \frac{b}{r^3}}{[F_k + F_d]}$$

Rogers and Yau (1989)

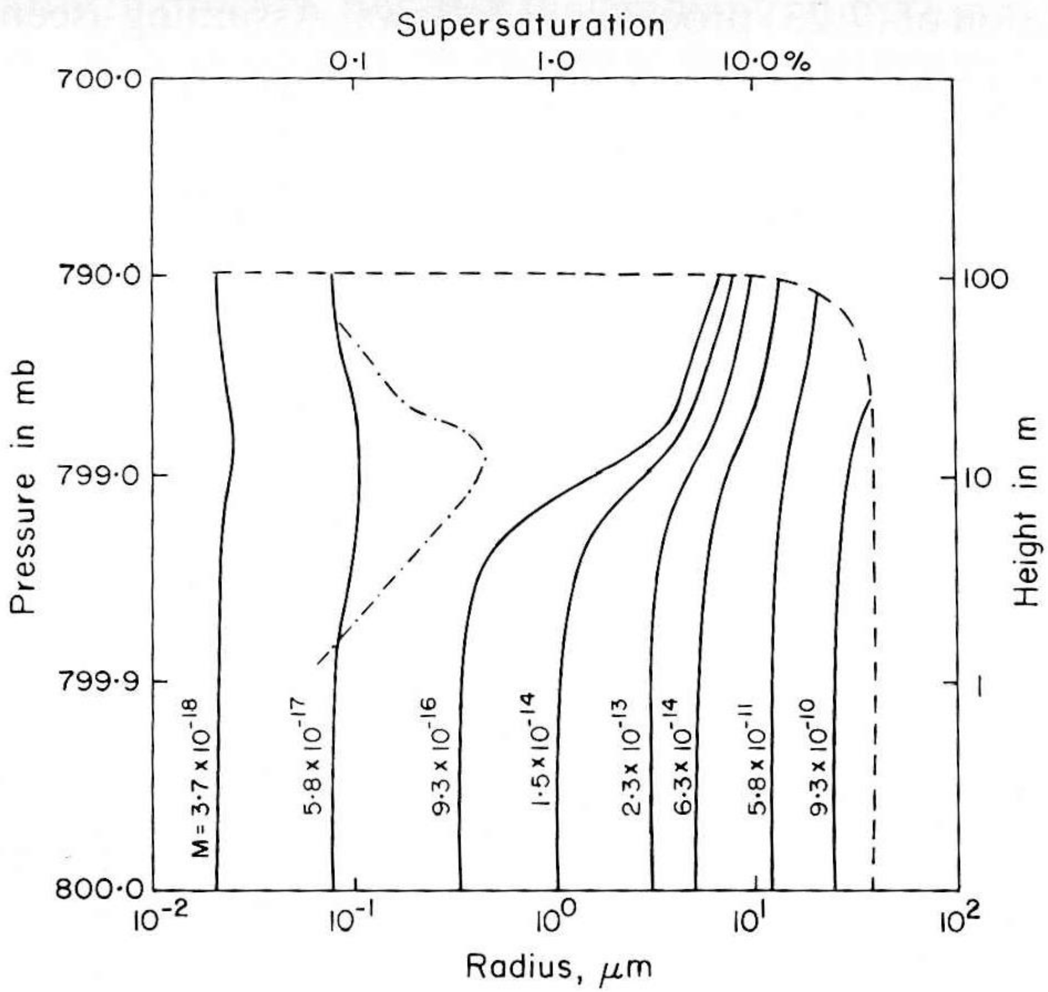

FIG. 7.3. Initial formation of cloud droplets and the variation of supersaturation above cloud base. (Adapted from Mordy, 1959.)

$N_{CCN}(SS) = C(SS)^k$, $C = 650\ cm^{-3}$, $k=0.7$, $U = 0.5$ and $2.0\ m\ s^{-1}$

larger U→higher SS

higher SS→higher N

larger U→higher N
→smaller r for similar LWC

larger U→shorter growth time to reach the same h
→slightly smaller LWC

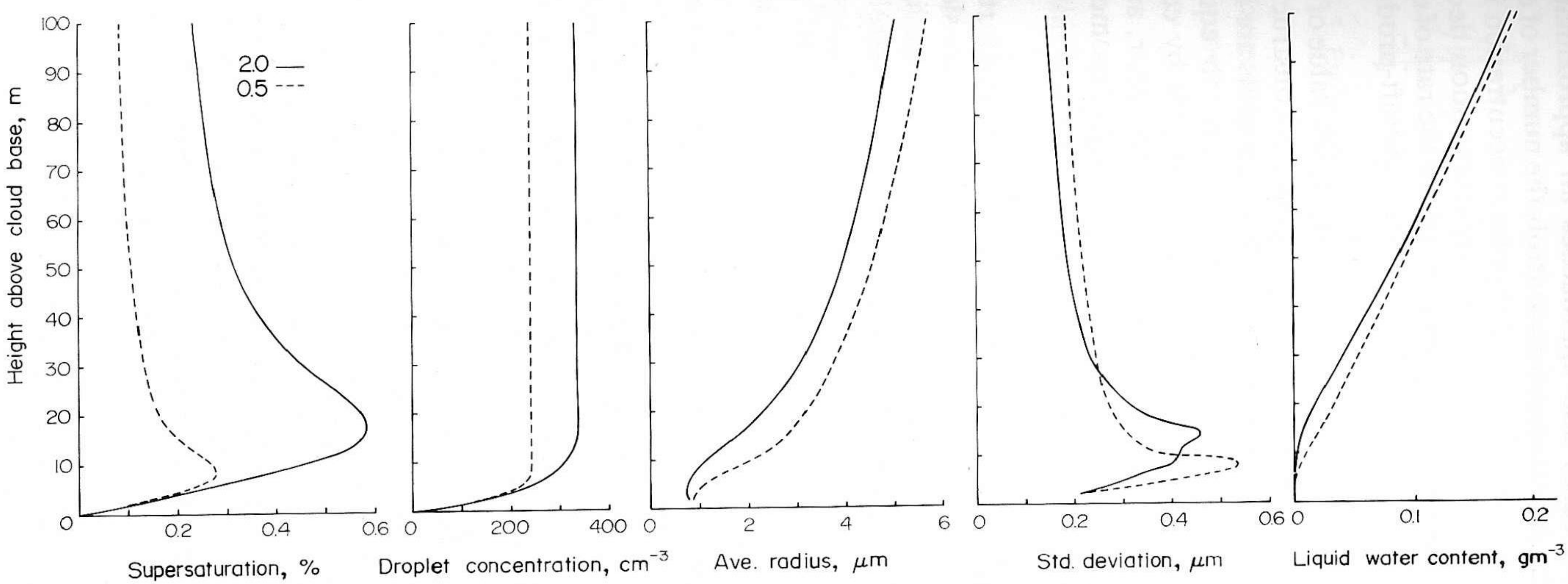

FIG. 7.4. Early development of cloud properties in air ascending at constant velocity of 0.5 m/s or 2 m/s.

Rogers and Yau (1989)

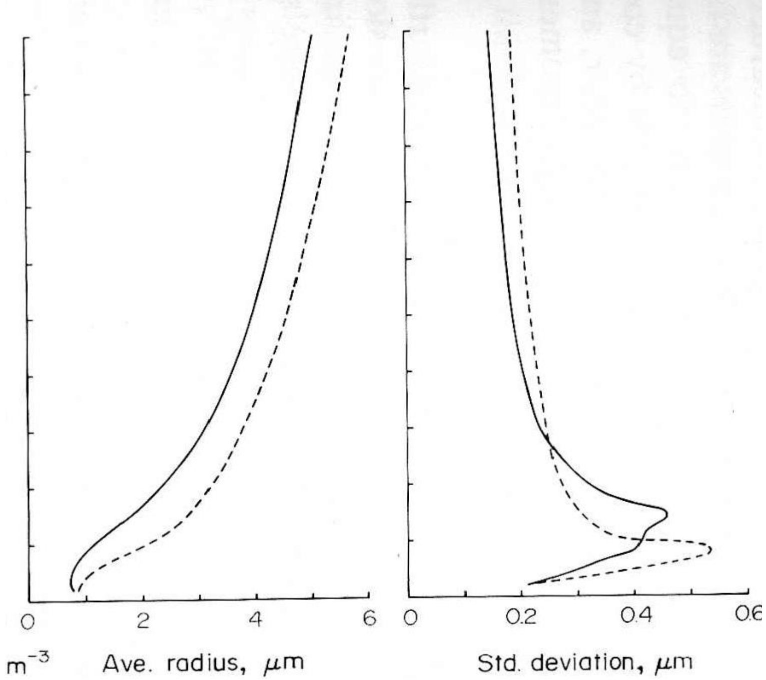

Usually observed droplet spectrum broadens as droplets grow with altitude!!!

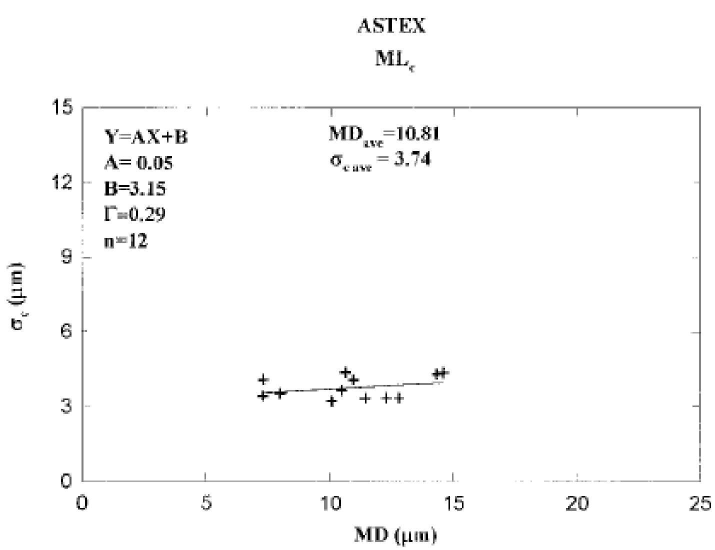

FIG. 5. As in Fig. 2 but only for those ASTEX soundings that displayed a monotonic increase in L_c with h (ML$_c$).

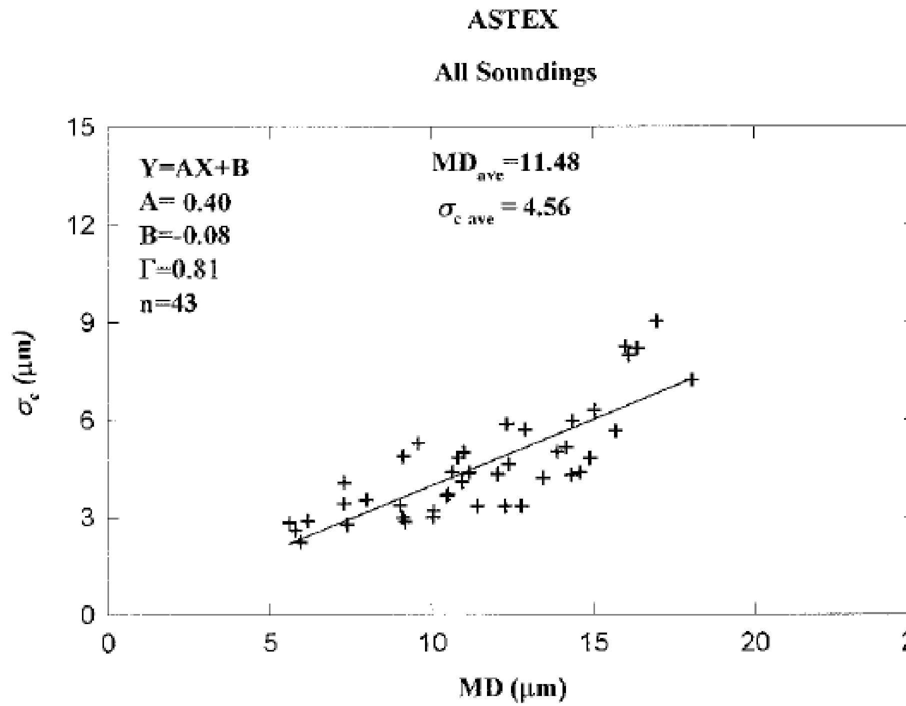

FIG. 2. Standard deviation (σ_c) and mean diameter (MD) of the droplet spectrum from the FSSP (d < 50 μm) averaged for each of the NCAR Electra vertical soundings in ASTEX: A and B are the slope and intercept of the linear regression, Γ is the correlation coefficient, and n is the number of data points.

Hudson and Yum (1997)

Comparison of theoretical prediction at 200 m from cloud base and observation from horizontal penetration

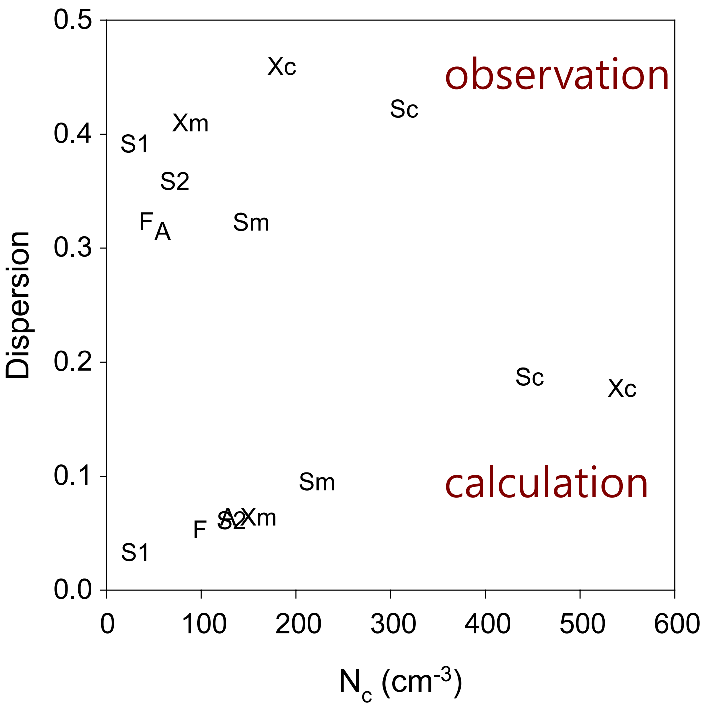

Yum and Hudson (2005)

ACE 1

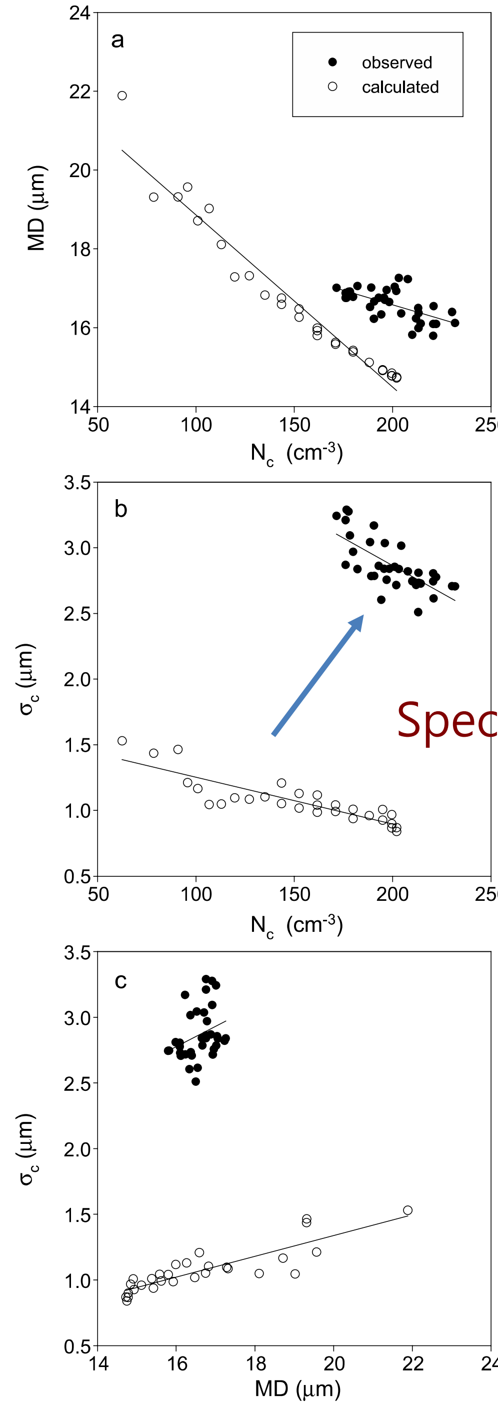

Spectral broadening!

Setting the stage for collision & coalescence

Giant nuclei: equil. size of giant soluble (deliquesced) particles may exceed r of 20 μm. ex) NaCl particles of SS_c=0.002% has r_s=1.4 μm and equil. radius at RH=100% is r_e=21 μm. Insoluble particle of r > 20 μm can also be involved in coalescence process immediately.

Entrainment and Mixing

Homogeneous mixing
Inhomogeneous mixing
Entity mixing

Turbulence enhanced broadening during condensational growth (i.e., stochastic condensational growth)

Turbulence enhanced collision

MIXING SCENARIOS

Homogeneous mixing (HM): when $\tau_e >> \tau_m$

All droplets in the mixed parcel experience the same degree of evaporation.

Inhomogeneous mixing (IM): when $\tau_e << \tau_m$

Droplets of the cloudy air adjacent to entrained air completely evaporate while the droplets in the remaining portion experience no evaporation.

τ_e : time for complete evaporation of a droplet

$$\tau_e = \frac{-D^2(F_k + F_d)}{8(S-1)}$$

τ_m : time for complete homogenization of a mixed parcel

$$\tau_m = \left(\frac{l_E^2}{\varepsilon}\right)^{1/3}$$

Homogeneous mixing (HM)

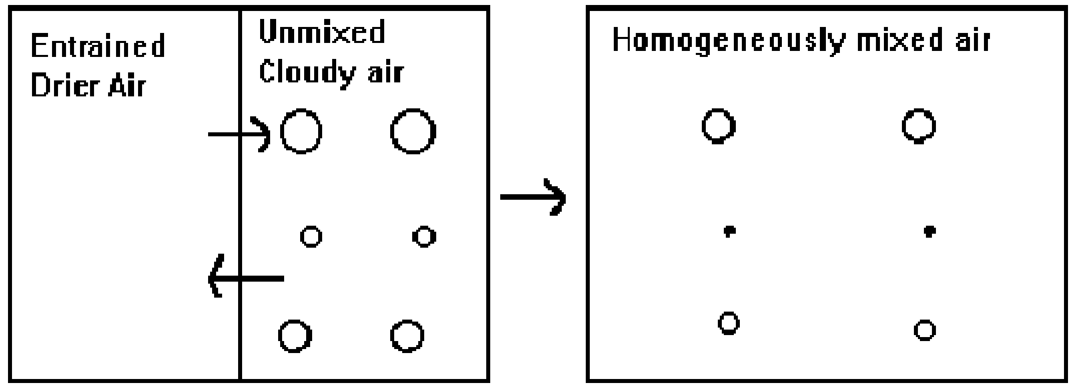

Inhomogeneous mixing (IM)

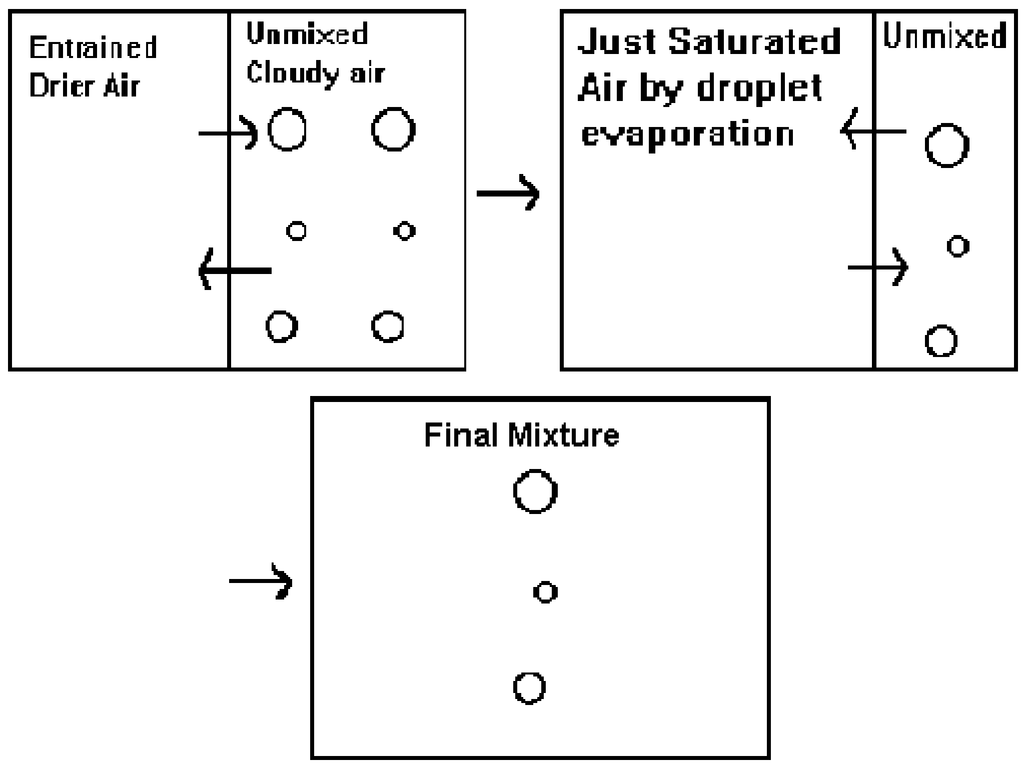

MIXING DIAGRAM

Effect of entrainment and mixing on cloud microphysics can be expressed as **relative deviation from the adiabatic values**.

$L = (\pi N D_v^3)/6 = NV$
$L_a = (\pi N_a D_{va}^3)/6 = N_a V_a$
$\alpha = L/L_a = (N/N_a)(D_v^3/D_{va}^3) = (N/N_a)(V/V_a)$

L: cloud droplet liquid water content (LWC)
N: cloud droplet number concentration
D_v: volume mean diameter of cloud droplets ($\pi D_v^3/6 = V$)
L_a, N_a, D_{va} and V_a: adiabatic values of L, N, D_v and V
α: LWC dilution ratio

HM: N decreases due to dilution and V decreases due to evaporation

IM: N decreases due to both dilution and complete evaporation of some of the droplets but V remains constant

$\alpha = L/L_a = NV/N_aV_a = (N/N_a)(V/V_a) = xy$. So $y = \alpha/x$ for a constant value of α

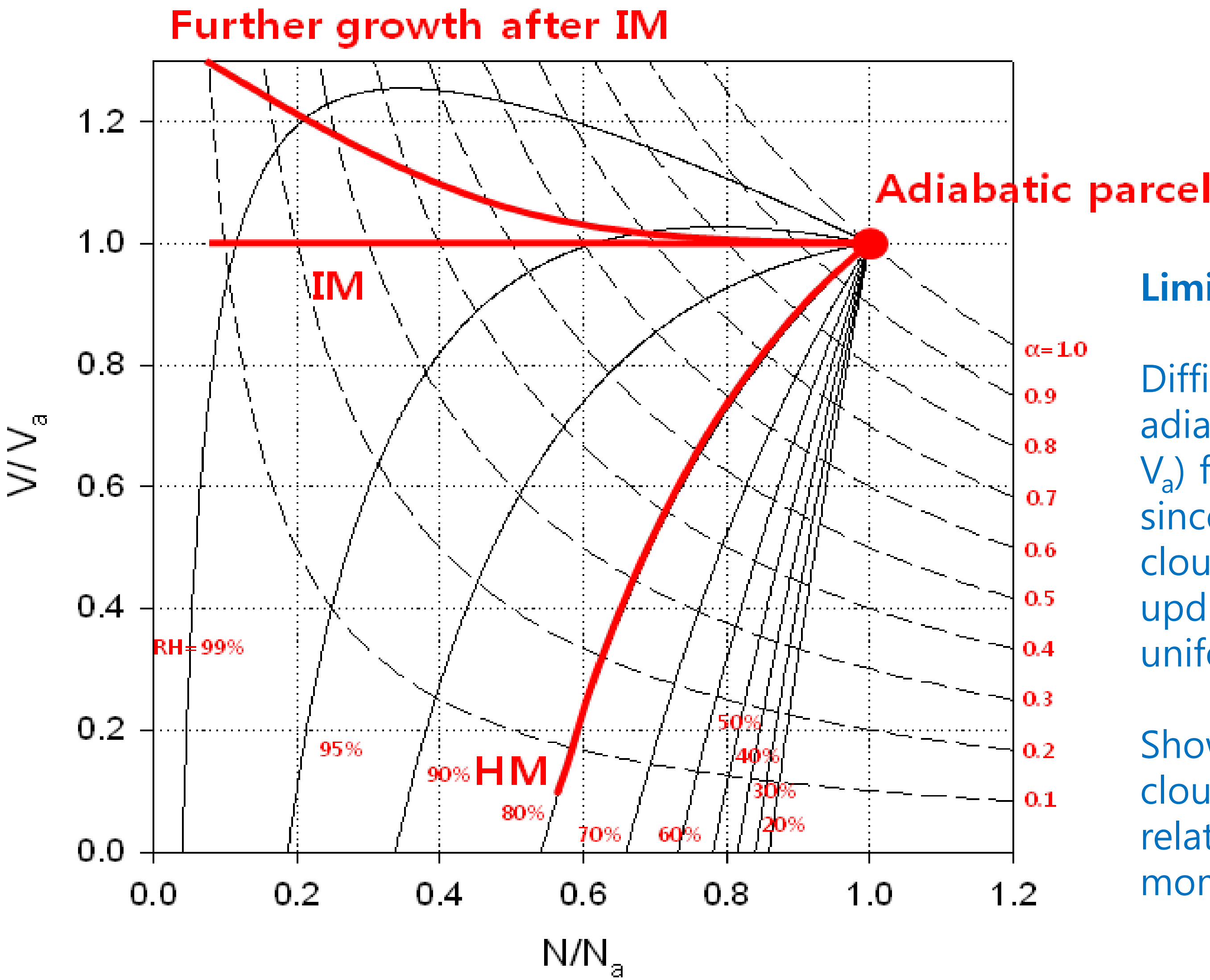

(Burnet and Brenguier, 2007)

Limitation

Difficult to find the adiabatic values (N_a and V_a) for a cloud segment since even for adiabatic clouds, they can vary if updraft speed is not uniform.

Shows only a snapshot of cloud microphysical relationships at the moment of measurement

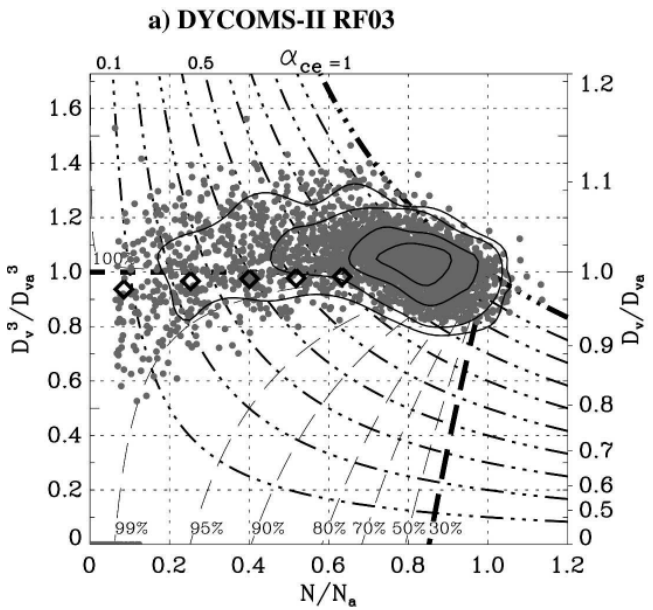

τ_e/τ_m = 0.05

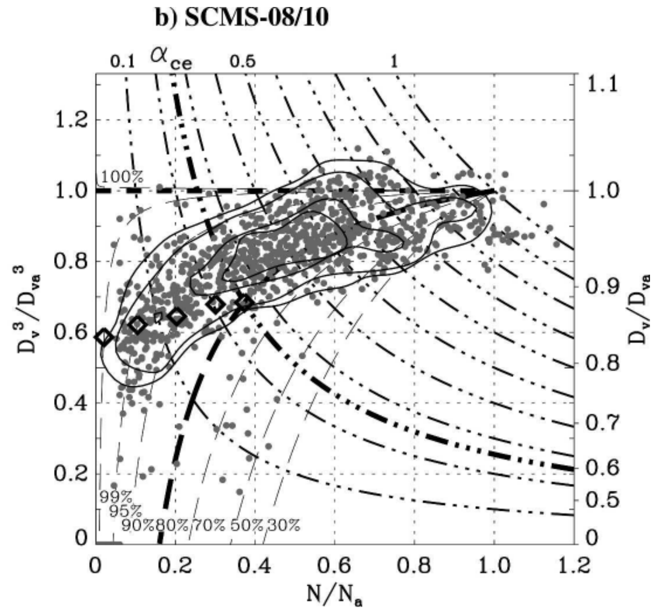

τ_e/τ_m = 6.6

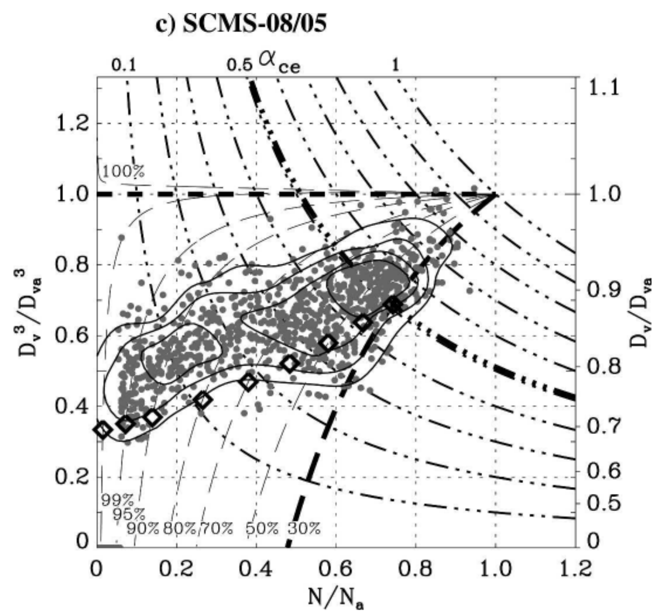

τ_e/τ_m = 1.9

FIG. 8. Scatterplot of $N - D_v^3$ for in situ–measured MVD and CDNC for the three cases. Isocontours of the frequency distribution are drawn for levels corresponding to 25%, 50%, 75%, and 90% of the data.

τ_e/τ_m : $1/D_a$
(D_a: Damkohler number)

Burnet and Brenguier (2007)

VAMOS (Variability of the American Monsoon System) Ocean Cloud Atmosphere Land Study

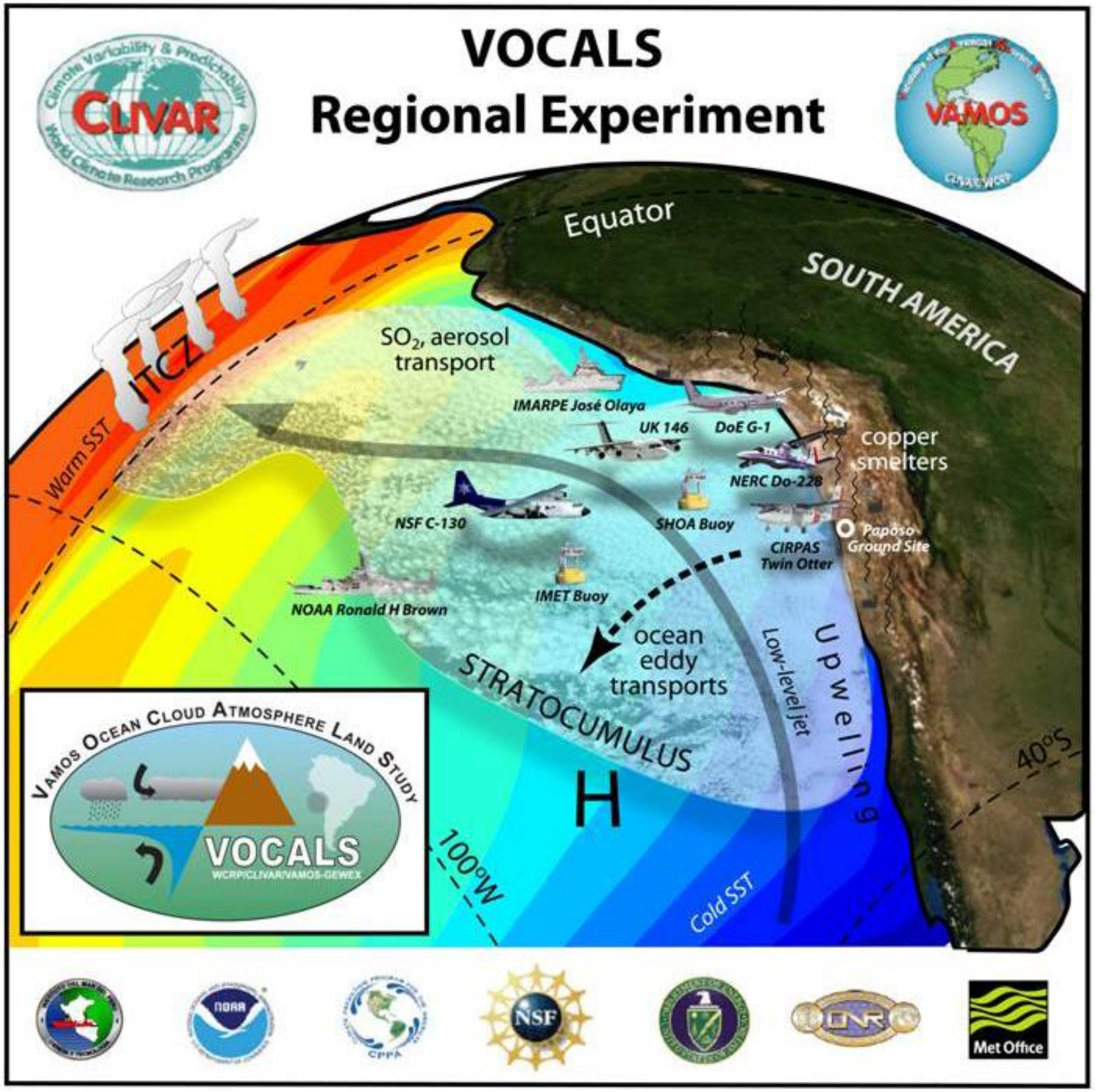

Oct.-Nov., 2008

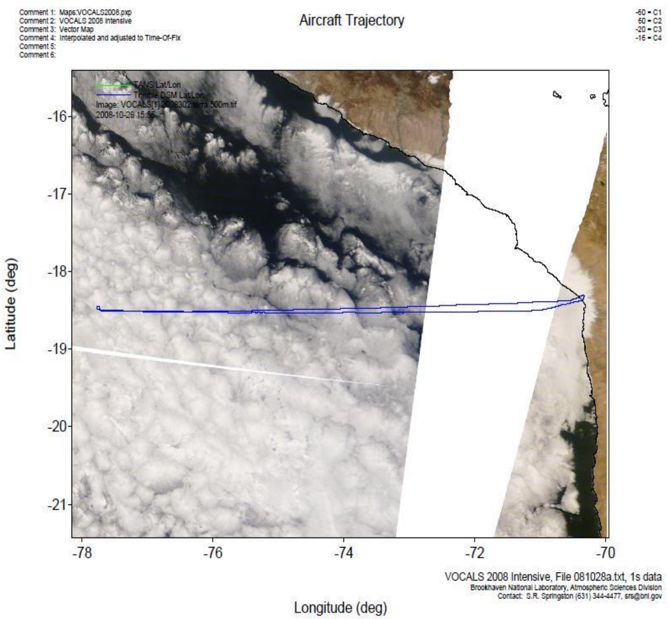

Yum et al. (2015)

The time variation of important cloud variables (O28)

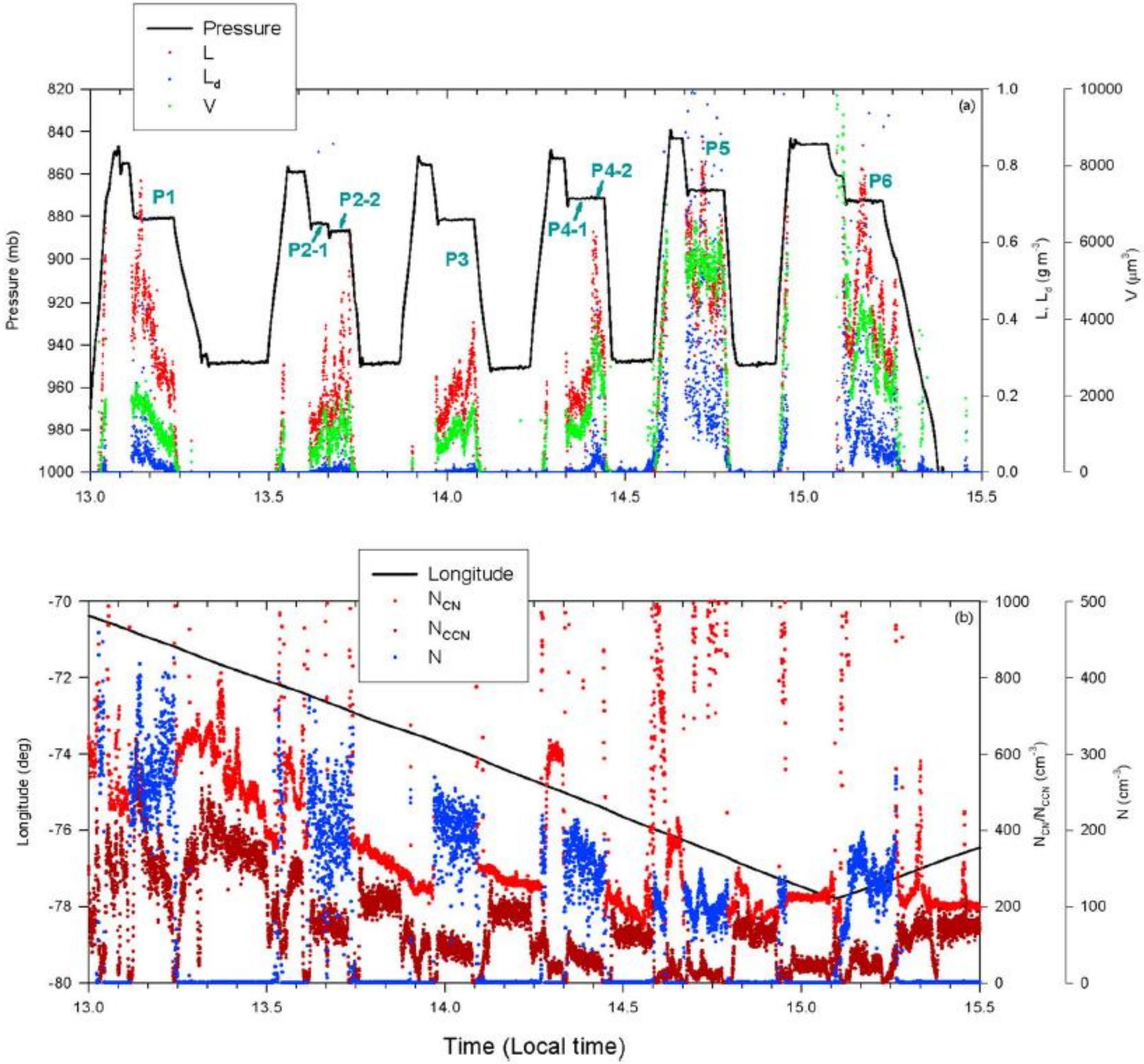

The vertical profiles of thermodynamic variables and L (O28)

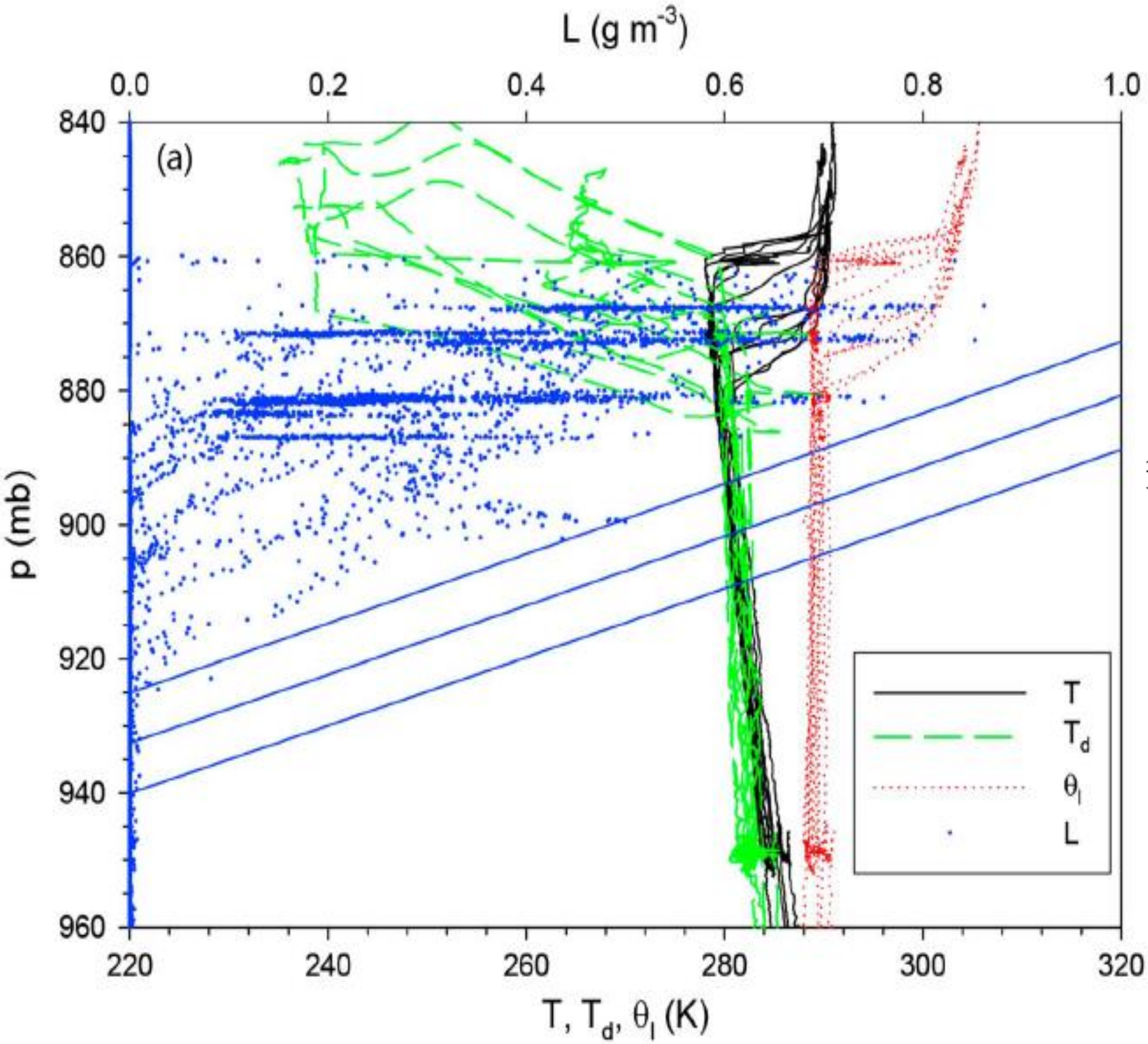

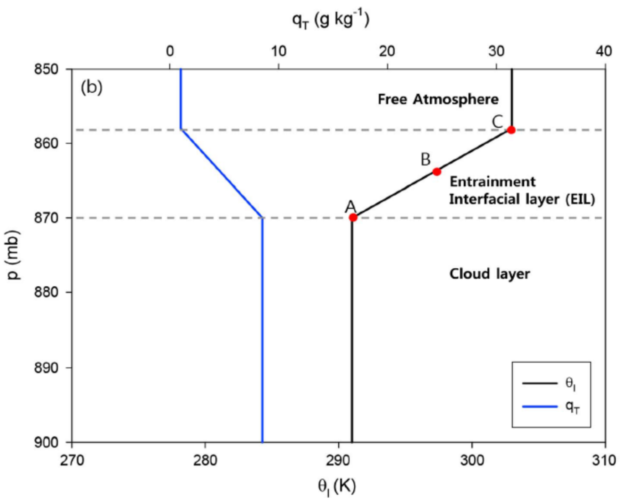

-Representative vertical profiles

Mixing diagram (1 Hz)

- Difficult to interpret!!

- Relative dispersion, ξ, generally increases as α decreases.

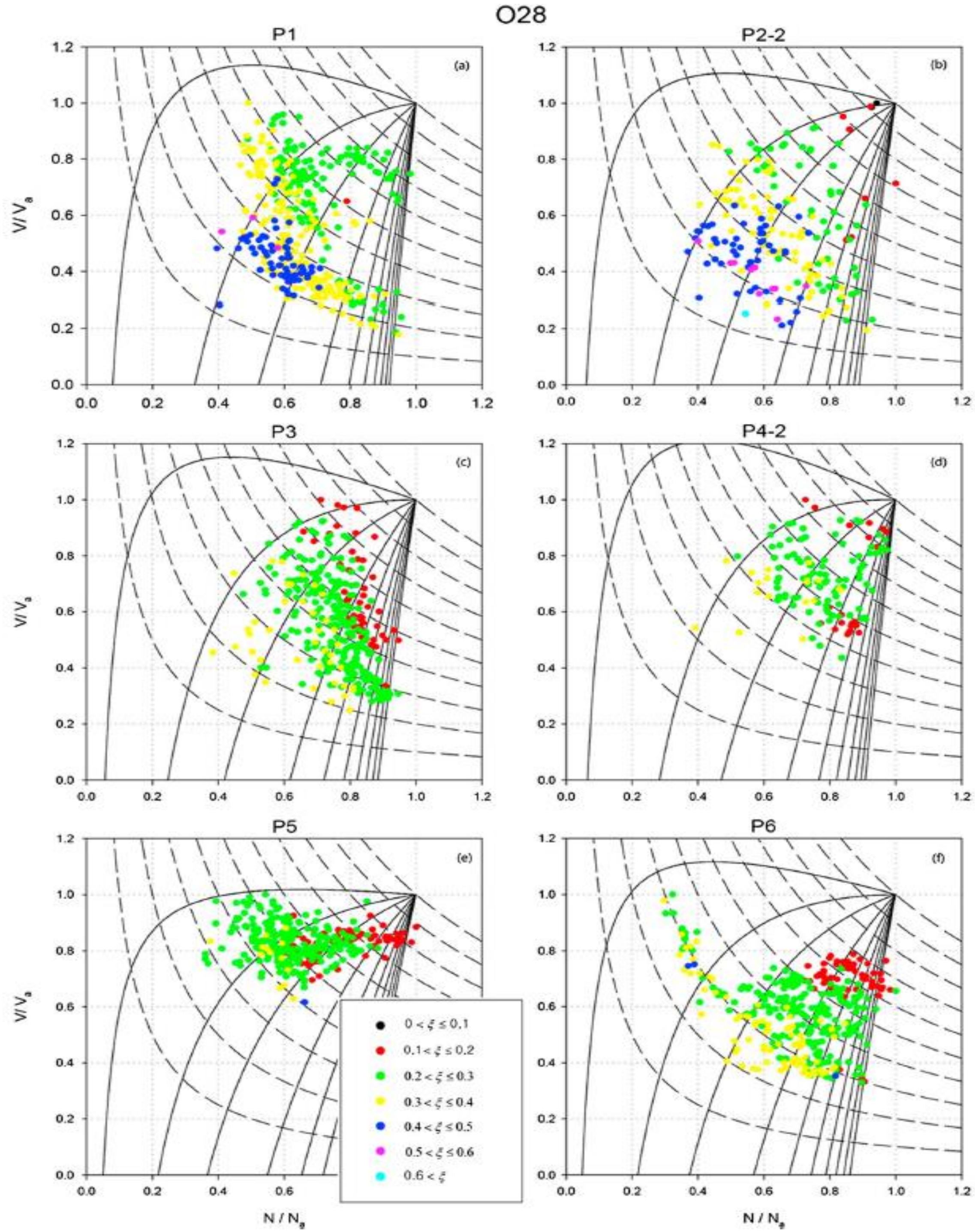

Frequently observed types of mixing diagram from O26 and O28
(20 s segments of 40 Hz data scatterplot and α bin plot)

O28

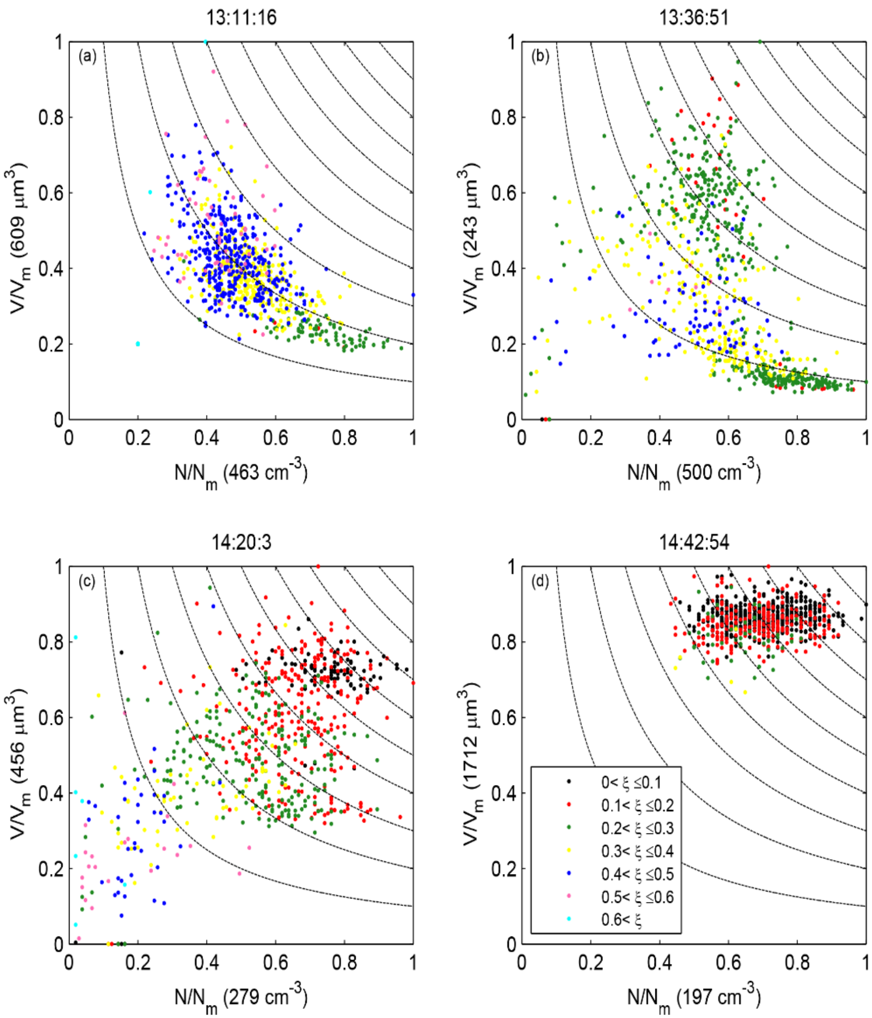

O28

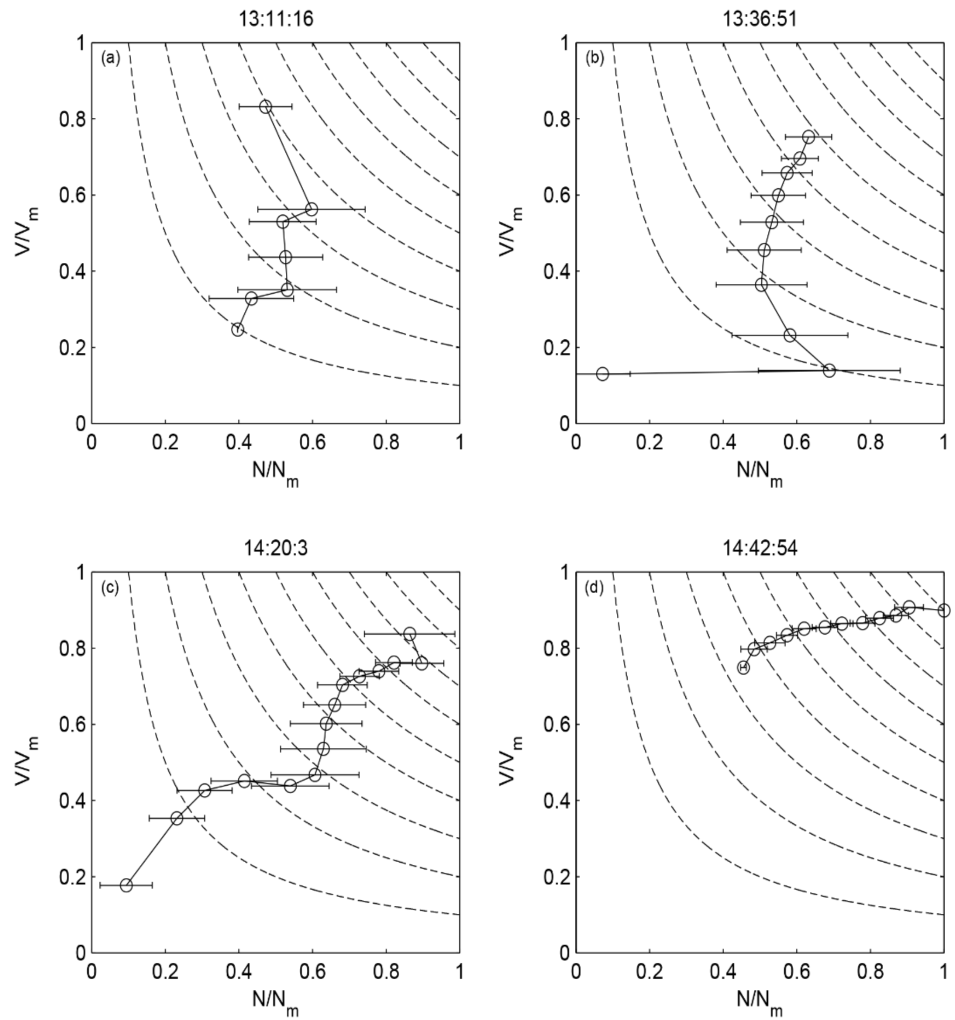

O28(P1)

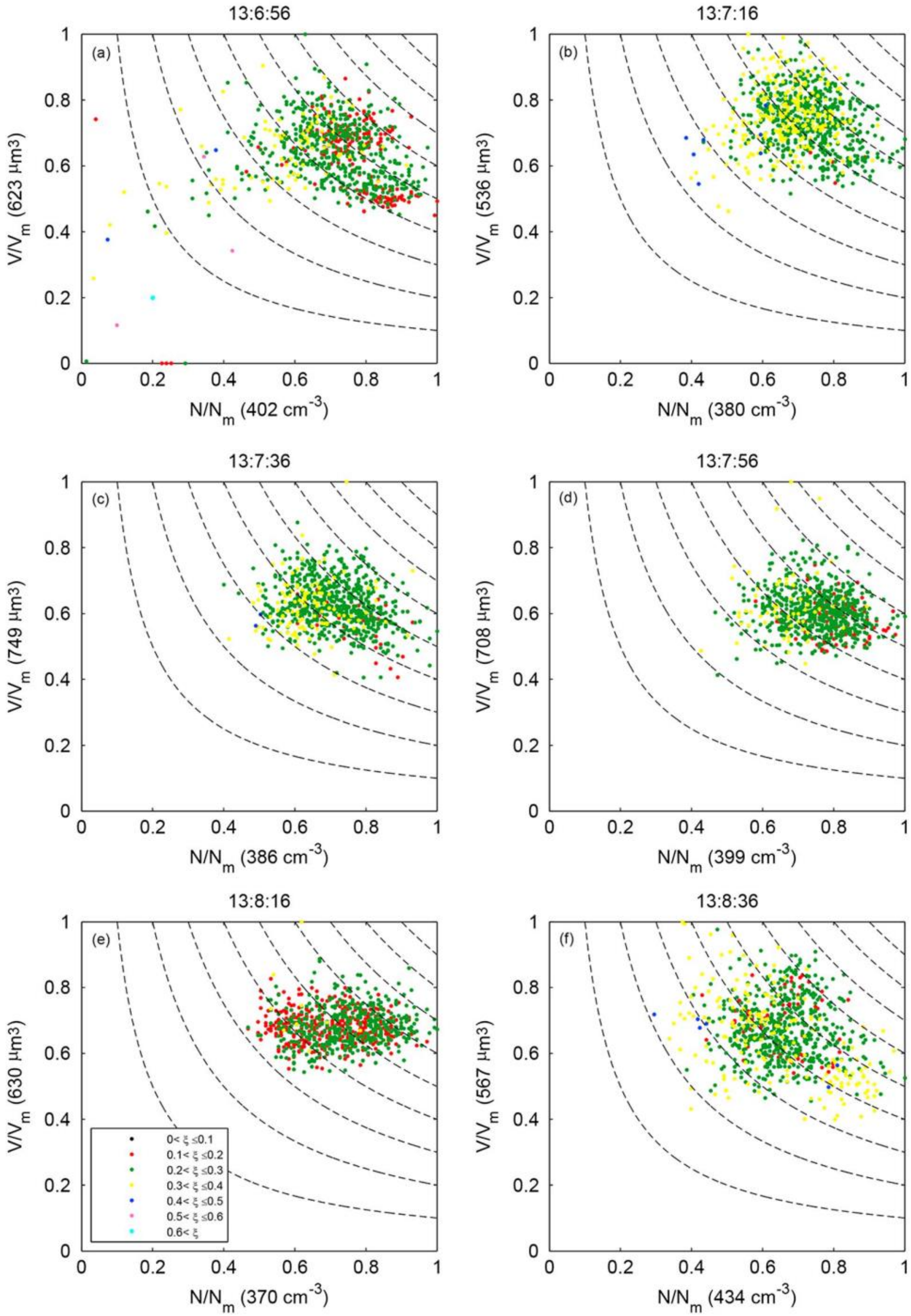

13:6:56
13:7:16
13:7:36
13:7:56
13:8:16
13:8:36
(a)
(b)
(c)
(d)
(e)
(f)
V/V_m (623 μm3)
V/V_m (536 μm3)
V/V_m (749 μm3)
V/V_m (708 μm3)
V/V_m (630 μm3)
V/V_m (567 μm3)
N/N_m (402 cm^-3)
N/N_m (380 cm^-3)
N/N_m (386 cm^-3)
N/N_m (399 cm^-3)
N/N_m (370 cm^-3)
N/N_m (434 cm^-3)
0< ξ ≤0.1
0.1< ξ ≤0.2
0.2< ξ ≤0.3
0.3< ξ ≤0.4
0.4< ξ ≤0.5
0.5< ξ ≤0.6
0.6< ξ

O28(P1)

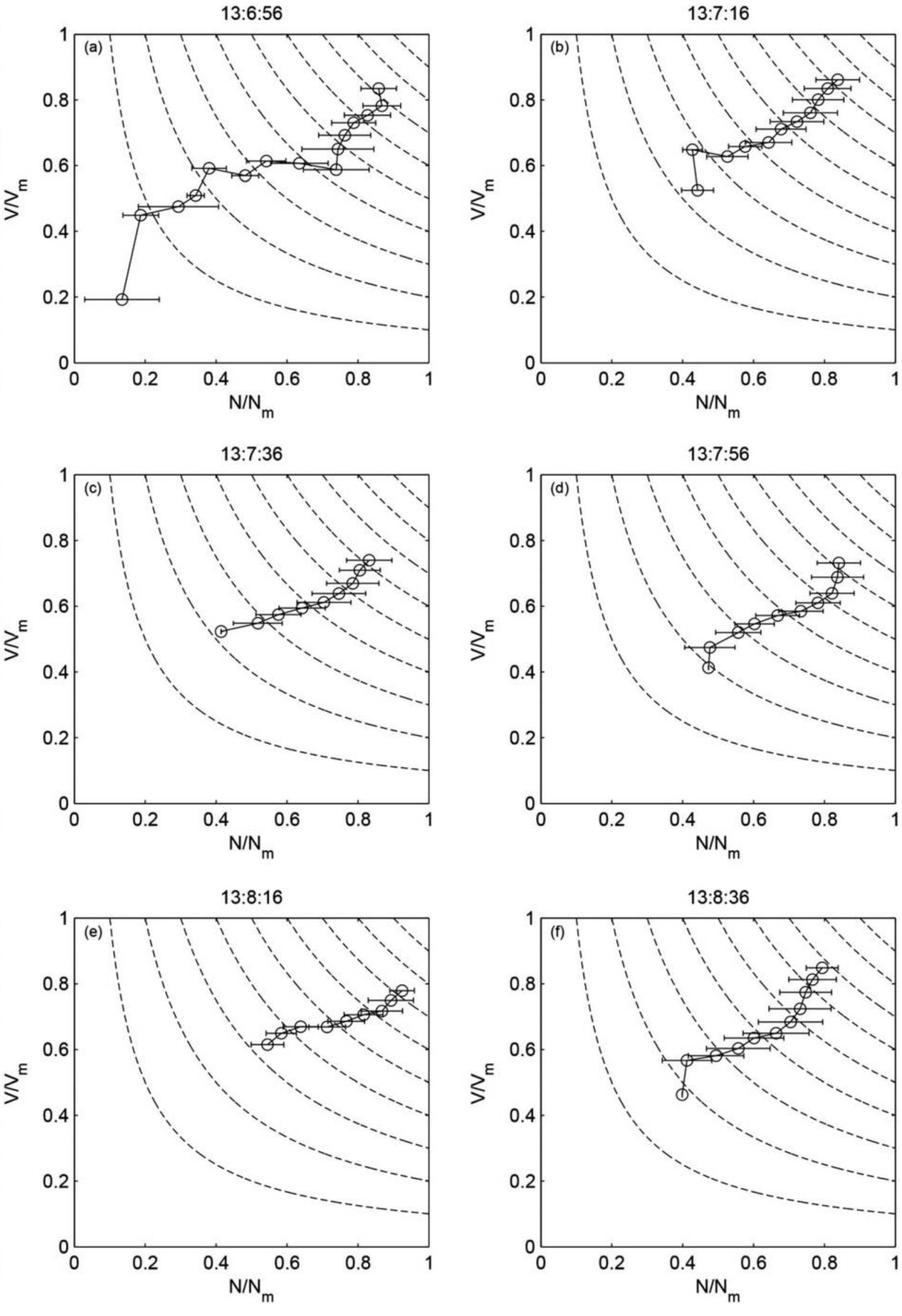

13:6:56
13:7:16
13:7:36
13:7:56
13:8:16
13:8:36
(a)
(b)
(c)
(d)
(e)
(f)
V/V_m
N/N_m

Expected correlations for some dominant cloud microphysical processes.

Dominant Process	$\Gamma_{N\text{-}V}$	$\Gamma_{N\text{-}L}$	$\Gamma_{V\text{-}L}$	No. of Segments
HM	>0	>0	>0	47
IM	~ 0	>0	~ 0	0
Further growth after IM	<0	>0	<0	10
Many recently activated droplets	<0	<0	>0	43
Small variation of L	<0	>0	>0	169
Not classified	•	•	•	34

[a]The dot in "not classified" indicates no preference for the sign of correlation coefficient.

- There are 47 segments that suggest HM.
- **No segment satisfies the criteria for IM**, but there are 10 segments that support further growth after IM.
- Small variation of L is the most frequently found cases.
- Important thing to note is that **positive relationship between V and L** is dominant for most of cloud segments.

Transition length scale (J*) and transition scale number (J_L)

- J^* indicates the length scale when the Damköhler number becomes 1 (Lehmann et al., 2009).

$$J^* = \varepsilon^{\frac{1}{2}} \tau_r^{\frac{3}{2}}$$

- J_L is the transition scale number, the ratio of J* to the Kolmogorov length scale (η) (Lu et al., 2011).

$$J_L = \frac{J^*}{\eta}$$

- The transition length and number strongly suggest **IM** for VOCALS clouds.

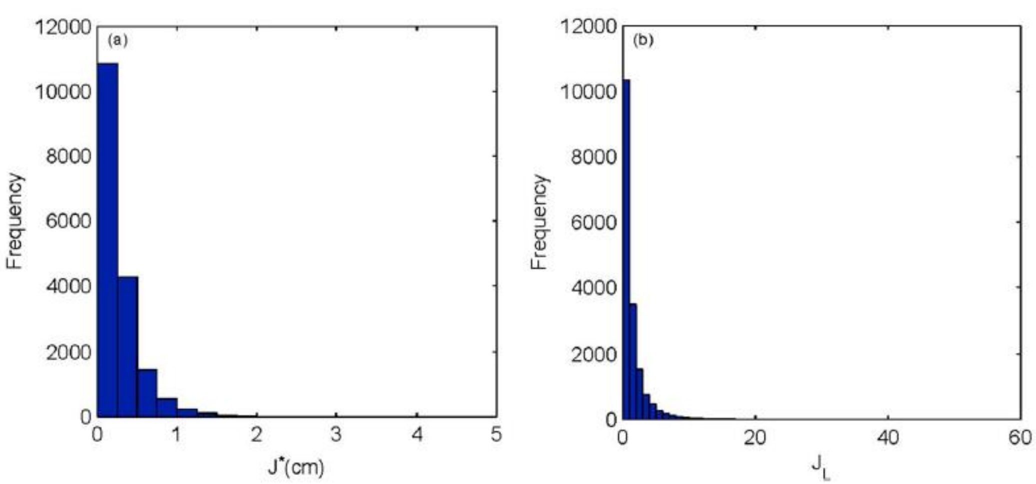

J^* (cm)	O26	Ave	5%	Median	95%
	P1	0.021	0.002	0.013	0.065
	P2	0.085	0.007	0.054	0.266
	P3	0.135	0.021	0.104	0.356
	P4	0.043	0.002	0.031	0.126
	O28				
	P1	0.275	0.043	0.190	0.795
	P2-1	0.193	0.019	0.122	0.596
	P2-2	0.260	0.041	0.183	0.742
	P3	0.141	0.023	0.106	0.375
	P4-1	0.166	0.033	0.134	0.417
	P4-2	0.462	0.094	0.348	1.185
	P5	1.457	0.223	1.058	4.048
	P6	0.910	0.171	0.690	2.404
J_L	O26				
	P1	0.129	0.006	0.059	0.462
	P2	0.505	0.019	0.226	1.882
	P3	0.803	0.049	0.471	2.707
	P4	0.226	0.002	0.118	0.801
	O28				
	P1	1.503	0.107	0.761	5.282
	P2-1	1.074	0.052	0.524	3.915
	P2-2	1.383	0.098	0.722	4.792
	P3	0.779	0.055	0.440	2.556
	P4-1	0.933	0.079	0.573	2.996
	P4-2	2.883	0.237	1.607	9.345
	P5	9.860	0.557	4.956	34.317
	P6	5.873	0.467	3.346	19.776

	40 Hz			1 Hz		
	$\Gamma_{N\text{-}V}$	$\Gamma_{N\text{-}L}$	$\Gamma_{V\text{-}L}$	$\Gamma_{N\text{-}V}$	$\Gamma_{N\text{-}L}$	$\Gamma_{V\text{-}L}$
O17						
P1	−0.35 ± 0.40	0.88 ± 0.10	0.04 ± 0.38	−0.48	0.91	−0.09
P2	−0.51 ± 0.30	0.03 ± 0.47	0.76 ± 0.28	−0.33	0.21	0.84
O26						
P1	−0.14 ± 0.19 (−0.10 ± 0.32)	0.18 ± 0.16 (0.26 ± 0.36)	0.91 ± 0.11 (0.90 ± 0.11)	−0.03	0.18	0.97
P2	−0.15 ± 0.22 (−0.09 ± 0.28)	0.48 ± 0.26 (0.59 ± 0.29)	0.74 ± 0.15 (0.69 ± 0.18)	0.20	0.40	0.97
P3	−0.21 ± 0.32 (−0.10 ± 0.30)	0.66 ± 0.15 (0.73 ± 0.18)	0.53 ± 0.16 (0.55 ± 0.19)	−0.43	0.12	0.89
P4	−0.62 ± 0.05 (−0.35 ± 0.28)	−0.11 ± 0.11 (−0.13 ± 0.33)	0.82 ± 0.03 (0.79 ± 0.21)	−0.80	−0.53	0.90
O28						
P1	−0.30 ± 0.22 (−0.12 ± 0.27)	0.48 ± 0.27 (0.60 ± 0.23)	0.65 ± 0.09 (0.68 ± 0.16)	−0.34	0.14	0.87
P2-1	−0.29 ± 0.27 (−0.16 ± 0.37)	0.34 ± 0.29 (0.46 ± 0.38)	0.73 ± 0.08 (0.72 ± 0.17)	−0.65	−0.35	0.91
P2-2	−0.22 ± 0.35 (−0.17 ± 0.36)	0.55 ± 0.20 (0.57 ± 0.28)	0.61 ± 0.14 (0.64 ± 0.21)	−0.06	0.46	0.84
P3	−0.13 ± 0.17 (−0.04 ± 0.31)	0.64 ± 0.17 (0.70 ± 0.20)	0.63 ± 0.14 (0.63 ± 0.17)	−0.36	0.02	0.92
P4-1	0.06 ± 0.30 (0.05 ± 0.34)	0.83 ± 0.06 (0.82 ± 0.13)	0.54 ± 0.16 (0.57 ± 0.21)	−0.27	0.47	0.71
P4-2	−0.03 ± 0.27 (−0.06 ± 0.26)	0.78 ± 0.08 (0.80 ± 0.12)	0.55 ± 0.14 (0.50 ± 0.18)	0.04	0.66	0.77
P5	0.04 ± 0.18 (0.02 ± 0.22)	0.84 ± 0.10 (0.86 ± 0.09)	0.53 ± 0.09 (0.49 ± 0.19)	−0.06	0.79	0.57
P6	−0.18 ± 0.20 (−0.06 ± 0.21)	0.74 ± 0.17 (0.80 ± 0.12)	0.48 ± 0.08 (0.52 ± 0.17)	−0.26	0.66	0.54

- Unlike all other penetrations, P1 of O17 was close to cloud top !

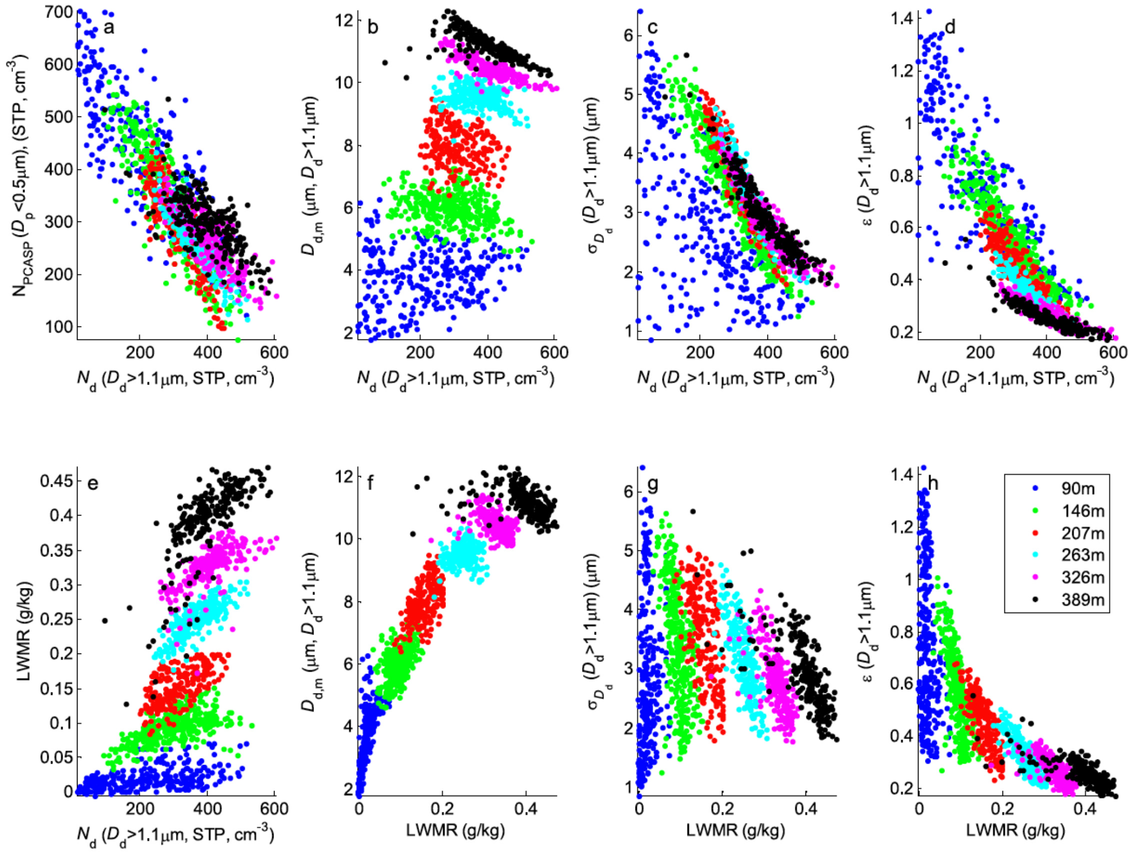

Wang et al. (2009)

Table 1. Correlation Coefficients Between Aerosol and Cloud Microphysics Calculated From 1 s Data as a Function of Sampling Altitude

Flight Date	Altitude (m)	γ $[N_{PCASP}, N_d]$	γ $[D_{d,m}, N_d]$	γ $[\sigma_{D_d}, N_d]$	γ $[\varepsilon, N_d]$	γ [LWMR, N_d]	γ $[D_{d,m}$, LWMR]	γ $[\sigma_{D_d}$, LWMR]	γ $[\varepsilon$, LWMR]	γ $[D_{d,top5}$, LWMR]	γ $[D_{d,top10}$, LWMR]
27 Jul 2005	389	−0.71	−0.71	−0.94	−0.92	0.74	−0.36	−0.74	−0.76	−0.43	−0.41
27 Jul 2005	326	−0.81	−0.83	−0.93	−0.90	0.67	−0.35	−0.67	−0.69	−0.51	−0.55
27 Jul 2005	263	−0.88	−0.32	−0.96	−0.93	0.79	0.18	−0.78	−0.84	−0.59	−0.56
27 Jul 2005	207	−0.87	−0.23	−0.95	−0.89	0.62	0.55	−0.56	−0.78	−0.33	−0.30
27 Jul 2005	146	−0.90	−0.26	−0.96	−0.92	0.63	0.49	−0.58	−0.74	−0.37	−0.23
27 Jul 2005	90	−0.81	0.15	−0.65	−0.84	0.48	0.68	0.11	−0.27	0.68	0.77
18 Jul 2005	276	−0.77	−0.79	−0.94	−0.88	0.85	−0.41	−0.83	−0.86	−0.62	−0.64
18 Jul 2005	155	−0.85	0.36	−0.84	−0.85	0.84	0.68	−0.60	−0.83	0.58	0.64
18 Jul 2005	60	−0.89	0.63	−0.20	−0.53	0.79	0.71	0.02	−0.36	0.77	0.74
20 Jul 2005	251	−0.50	−0.97	−0.89	−0.83	0.73	−0.71	−0.80	−0.79	−0.78	−0.76
20 Jul 2005	187	−0.21	−0.85	−0.93	−0.90	0.69	−0.39	−0.58	−0.60	−0.50	−0.49
20 Jul 2005	129	−0.59	0.15	−0.88	−0.86	0.54	0.80	−0.55	−0.64	−0.38	−0.30
20 Jul 2005	69	−0.93	0.56	−0.30	−0.73	0.72	0.84	0.20	−0.36	0.91	0.91

Vertical Circulation Mixing

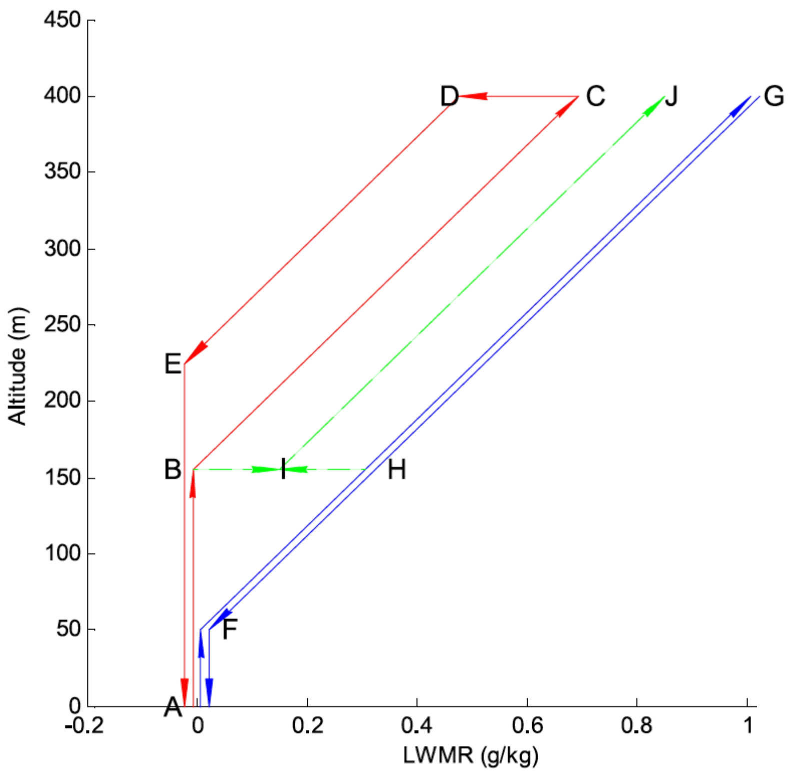

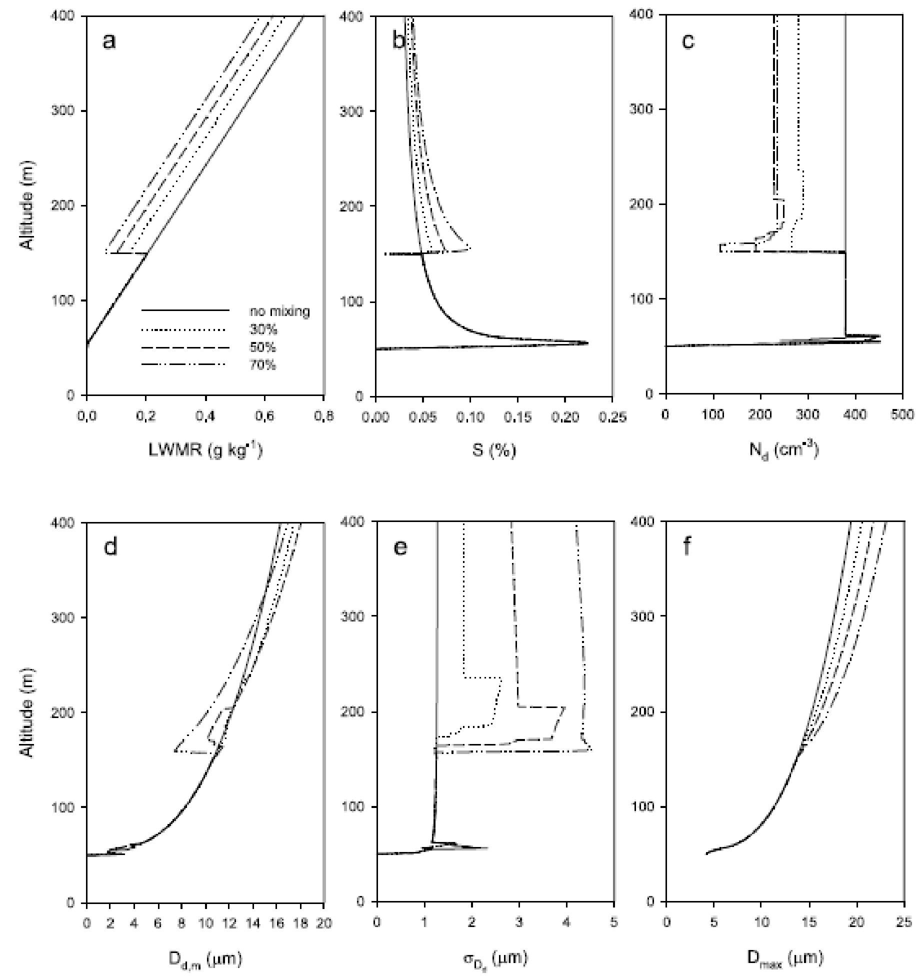

Figure 11. Modeled evolutions of (a) liquid water mixing ratio, (b) supersaturation, (c) droplet number concentration, (d) mean droplet diameter, (e) standard deviation of droplet diameter, and (f) the diameter of the largest droplet size bin for a LLCL cloud parcel and mixtures of the LLCL and HLCL cloud parcels with volume mixing ratio of 70:30, 50:50, and 30:70. The LLCL cloud parcel has a LCL of 50 m and is mixed with the HLCL parcel at its LCL of 150 m.

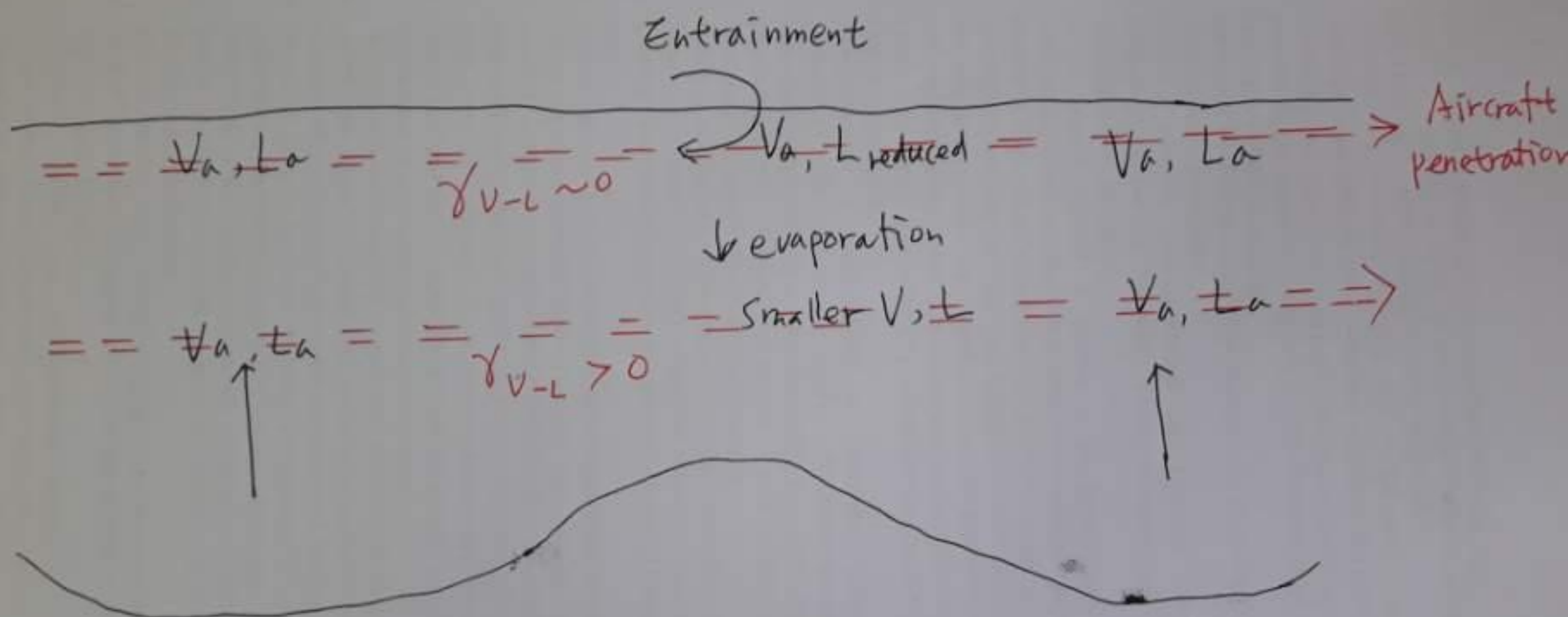
Entrainment
Aircraft penetration
Va, La
γV-L ~ 0
Va, L reduced
Va, La
evaporation
Smaller V, L
Va, La
γV-L > 0
Va, La

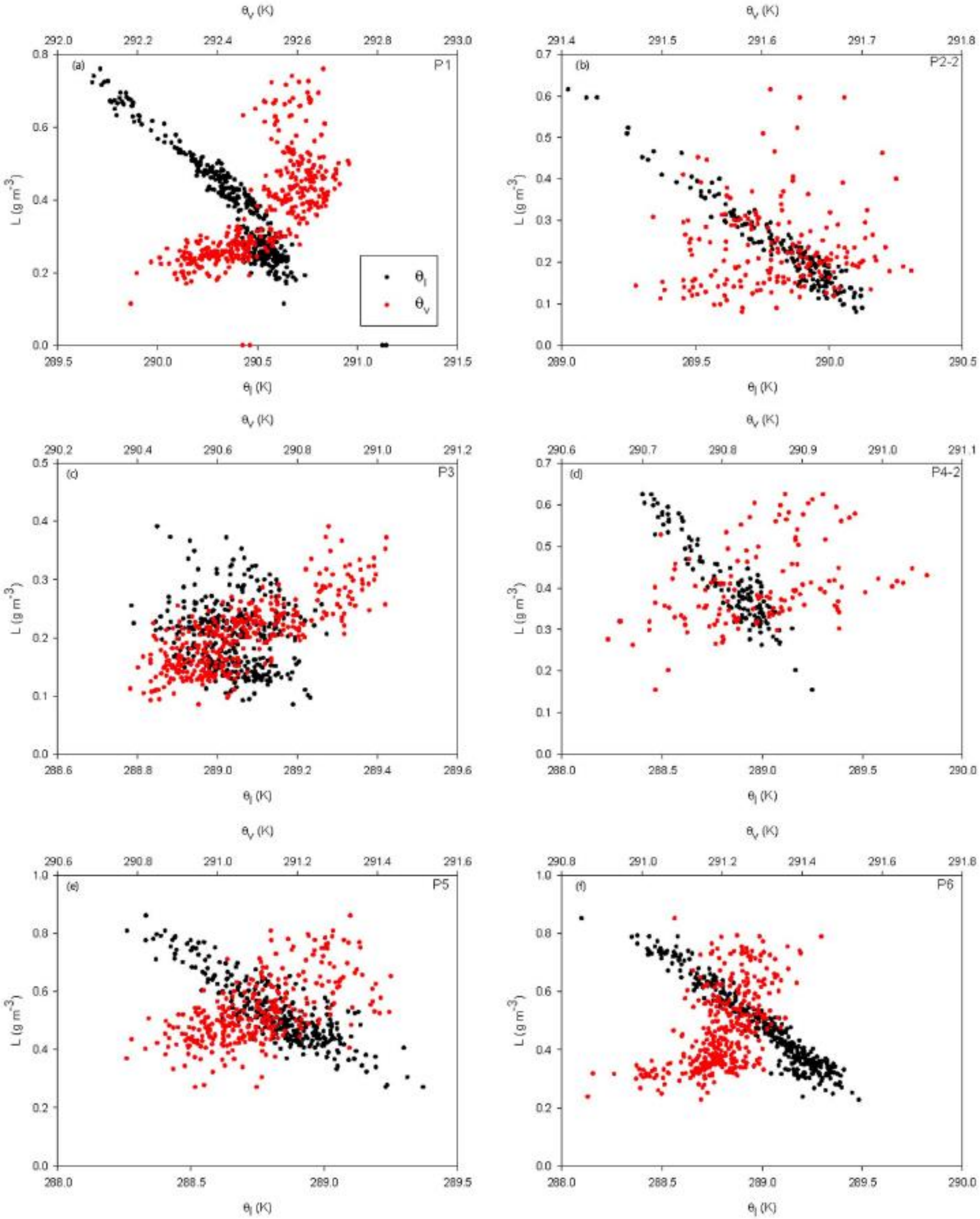

- $$\theta_l = \theta - \left(\frac{\theta}{T}\frac{L_v}{C_p}\right) q_l$$

-Liquid water potential temperature

- $$\theta_v = \theta(1 + 0.61 q_v - q_l)$$

-Virtual potential temperature

- CTEI criterion was satisfied in these clouds

CTEI criterion: $\left[\Delta\theta_e - \kappa\left(\frac{L_v}{C_p}\right)\Delta q_T < 0\right]$

Routine AAF Clouds with Low Optical Water Depths (CLOWD) Optical Radiative Observations (RACORO)

January-June, 2009

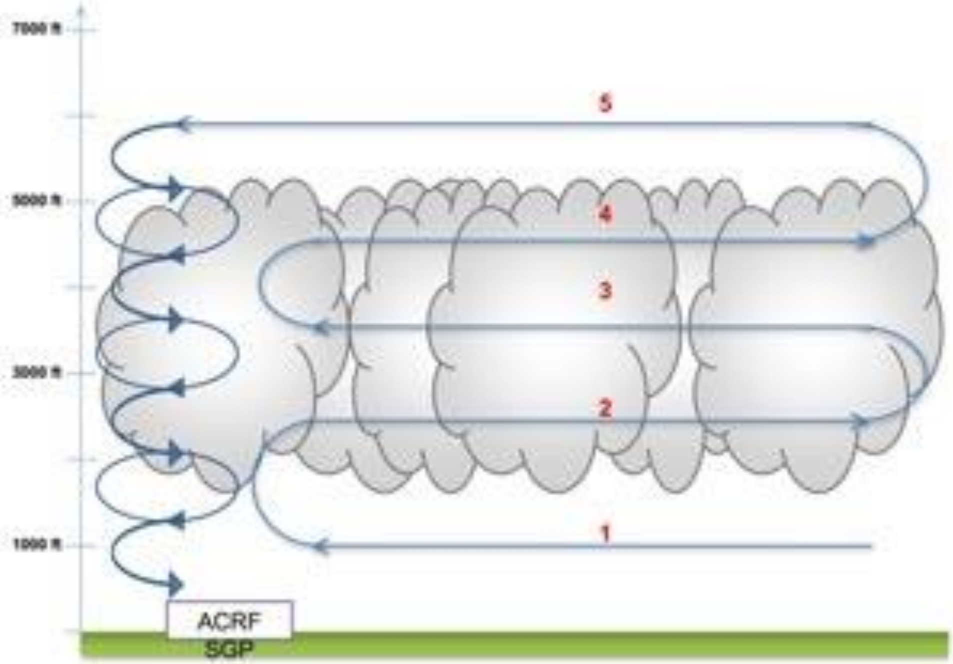

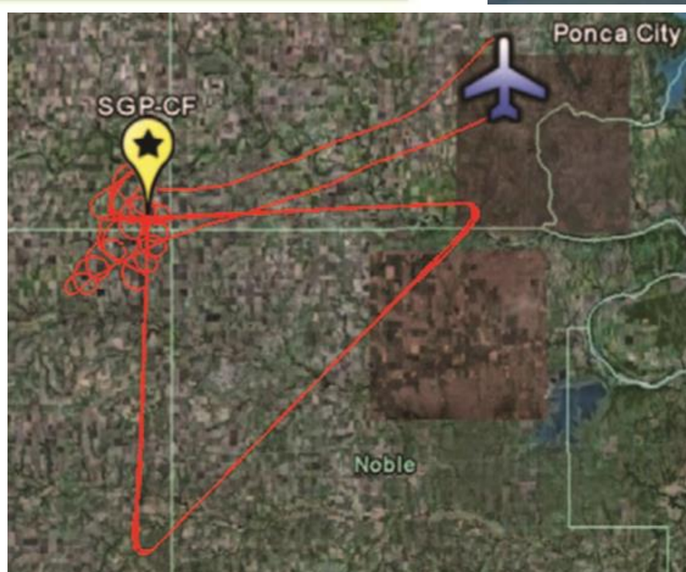

Yeom et al. (2017)

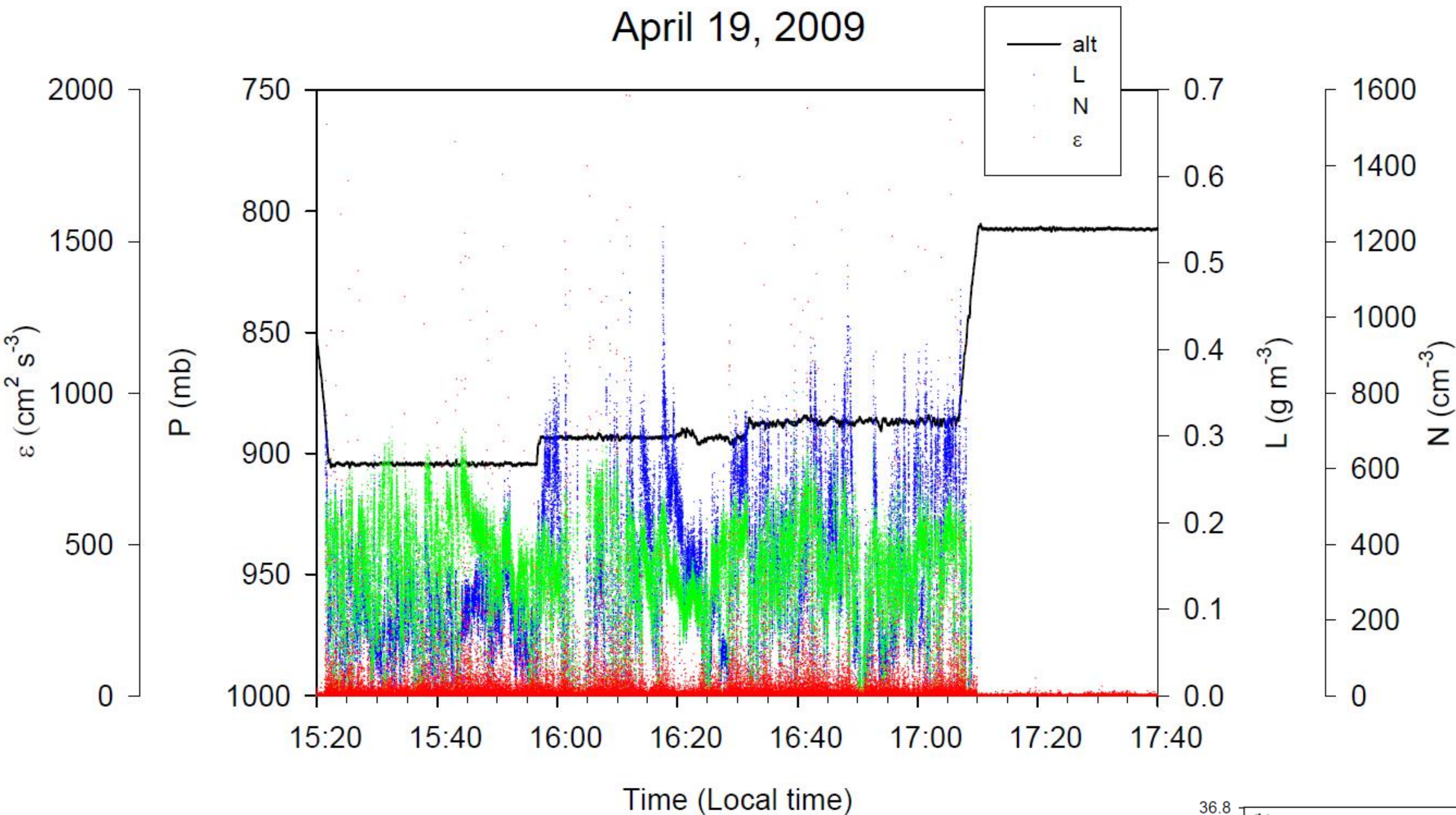
April 19, 2009
alt
L
N
ε
ε (cm^2 s^-3)
P (mb)
L (g m^-3)
N (cm^-3)
Time (Local time)
2000
1500
1000
500
0
750
800
850
900
950
1000
0.7
0.6
0.5
0.4
0.3
0.2
0.1
0.0
1600
1400
1200
1000
800
600
400
200
0
15:20
15:40
16:00
16:20
16:40
17:00
17:20
17:40

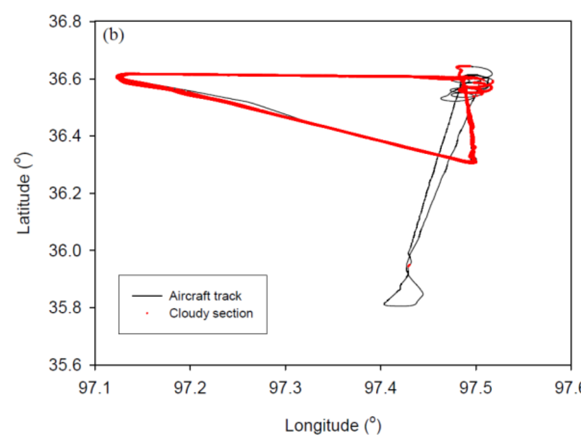
(b)
Aircraft track
Cloudy section
Latitude (°)
Longitude (°)
36.8
36.6
36.4
36.2
36.0
35.8
35.6
97.1
97.2
97.3
97.4
97.5
97.6

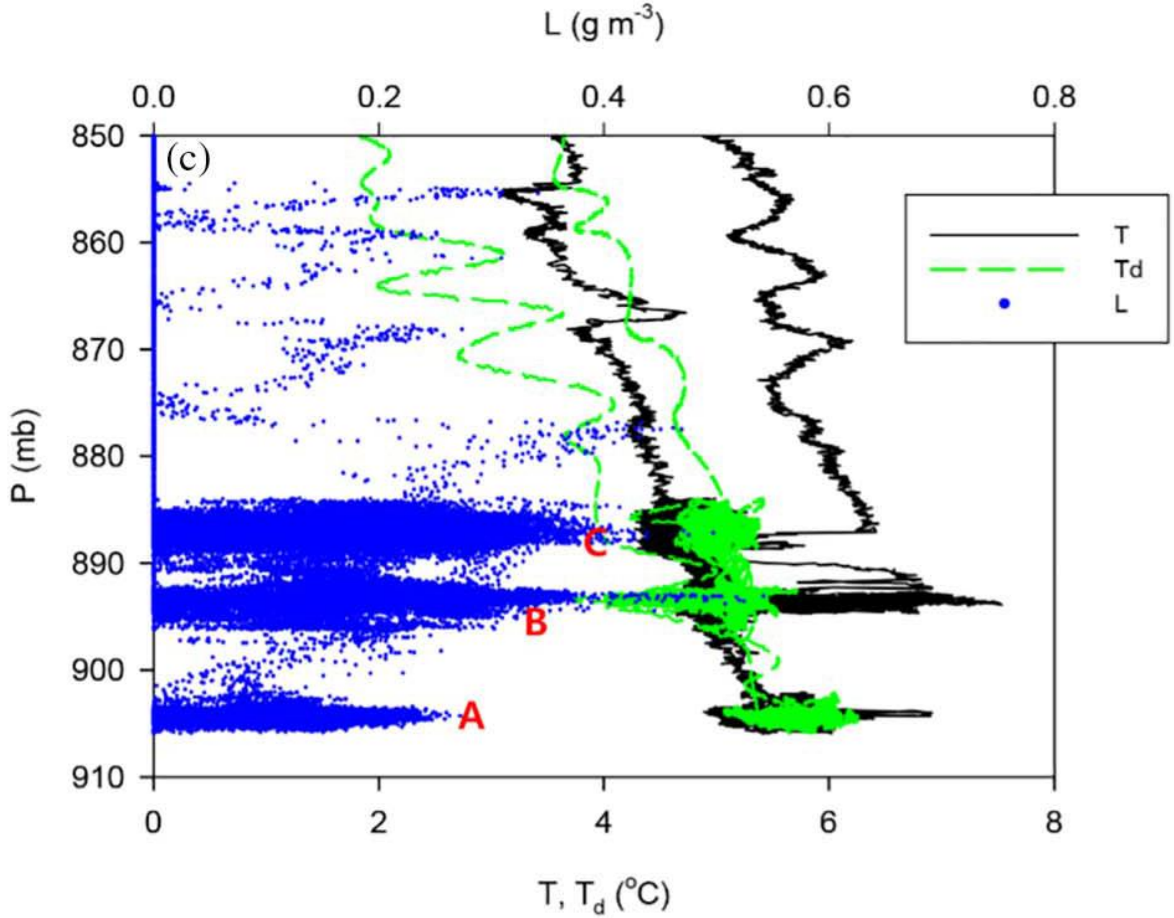

- The differences of T and T_d between in and above the clouds were much smaller compared to the VOCALS maritime stratocumulus clouds (Yum et al., 2015).

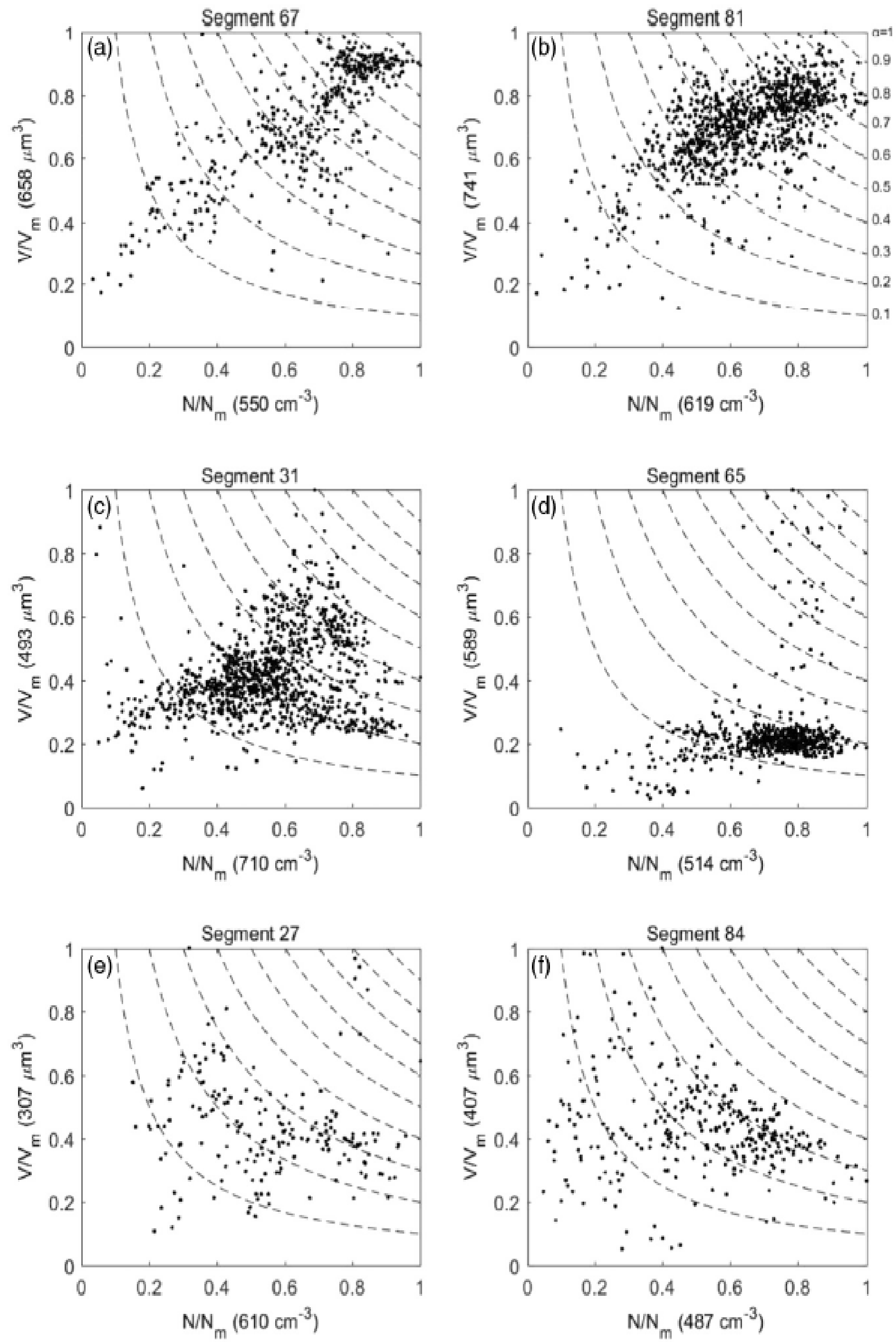

- **Most of the segments** show the data scatter similar to those shown in segments 67 and 81 as N/N_m decreases with the decrease of V/V_m, which clearly indicates **HM**.

Correlation Coefficients

Process	Γ_{N-V}	Γ_{N-L}	Γ_{V-L}	No. of segments
HM	> 0	> 0	> 0	93
IM	~ 0	> 0	~ 0	0
Small variation in L	< 0	> 0	> 0	13
Not classified	–	–	–	4

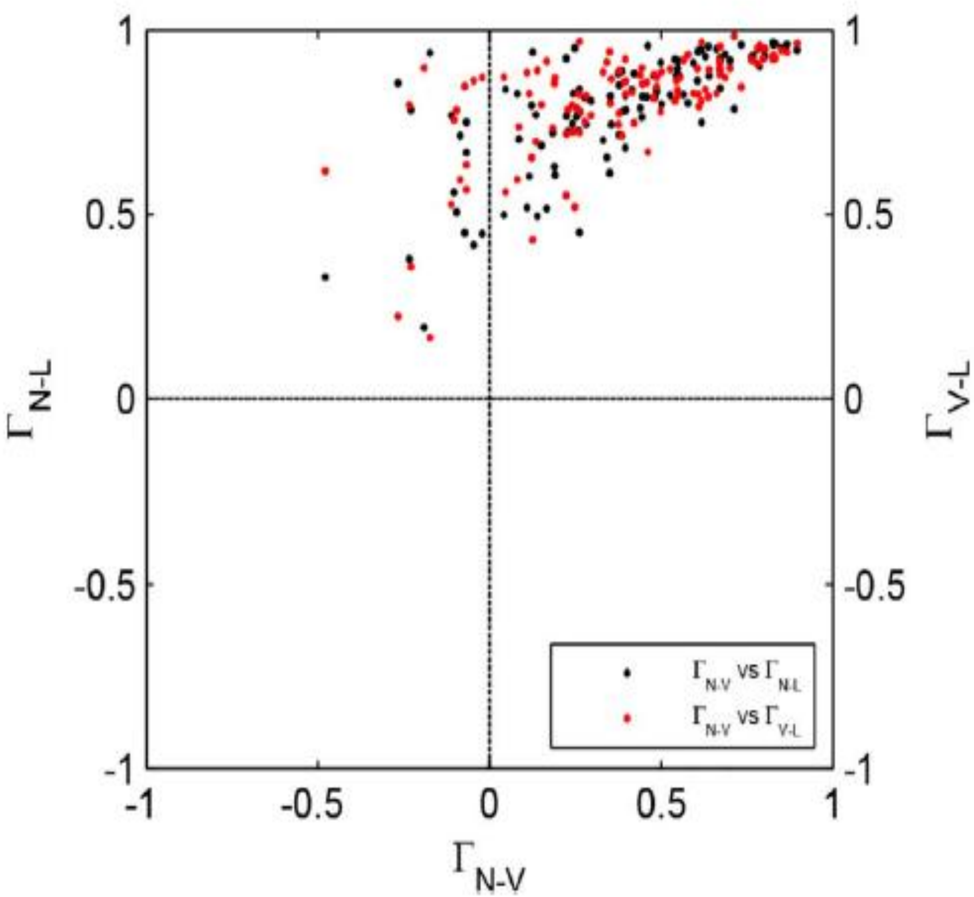

- Basically two patterns emerge dominantly for the 110 cloud segments (HM, Small variation in L).

- These correlation coefficient values strongly support the **HM.**

The transition length scale (L^*) and scale number (N_L)

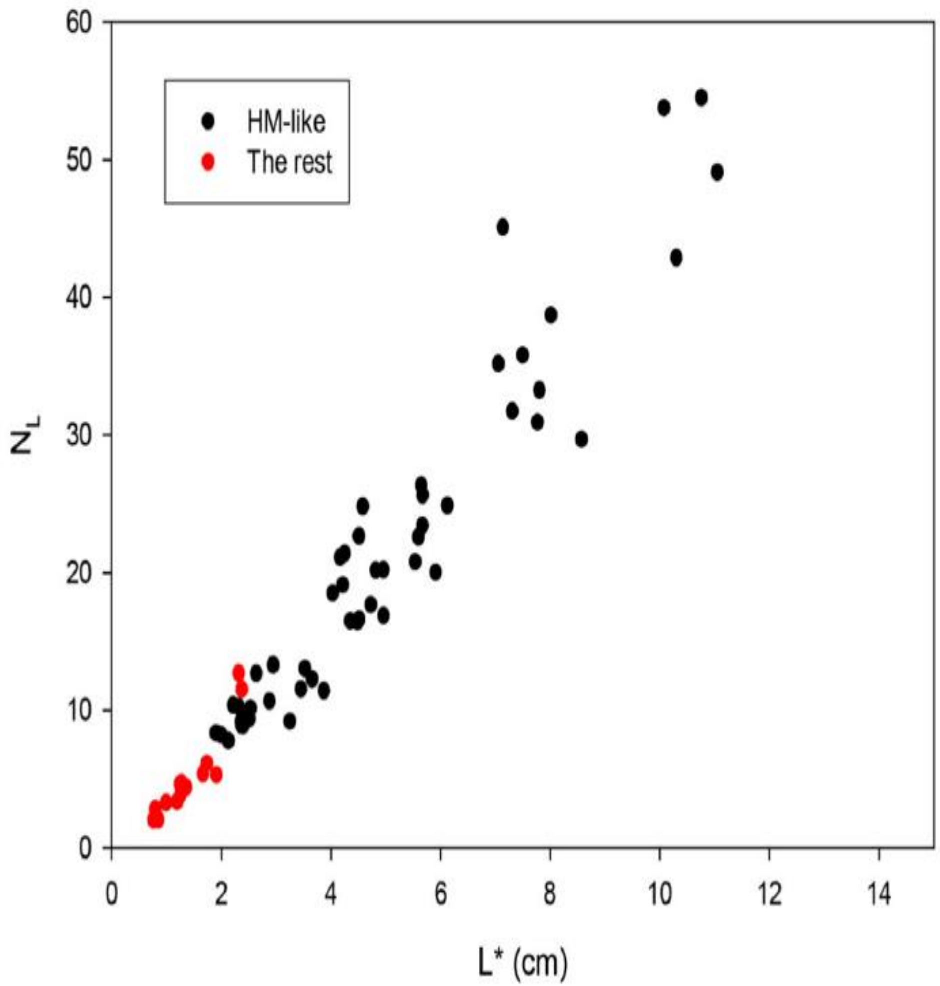

Segment number	67	81	31	65	27	84
Mean transition scale number (N_L)	35.2	33.3	4.7	2.3	4.4	5.3
Mean transition length (L^*) (cm)	7.1	7.8	1.3	0.7	1.4	1.7
Dominant process	HM	HM	Vaguely HM	Vaguely HM	Iso-α line	Iso-α line

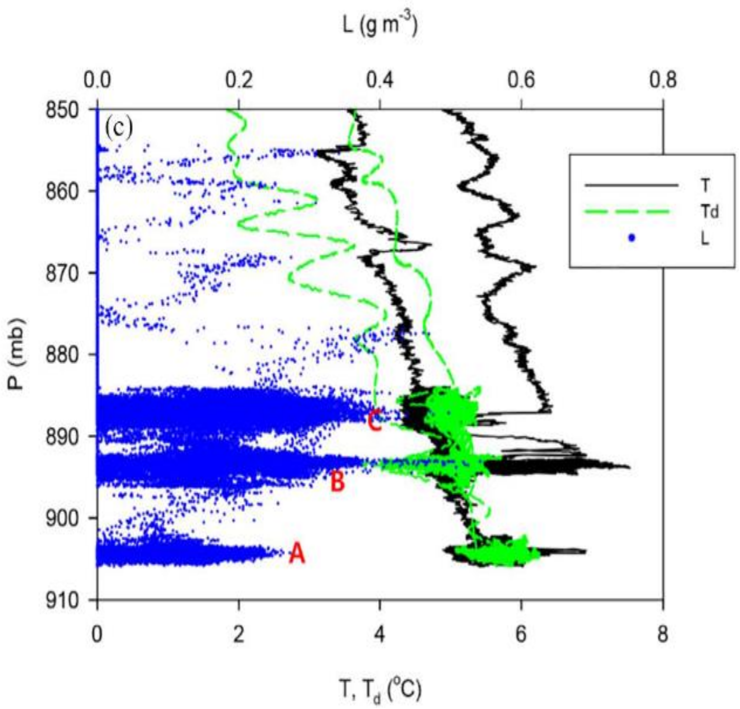

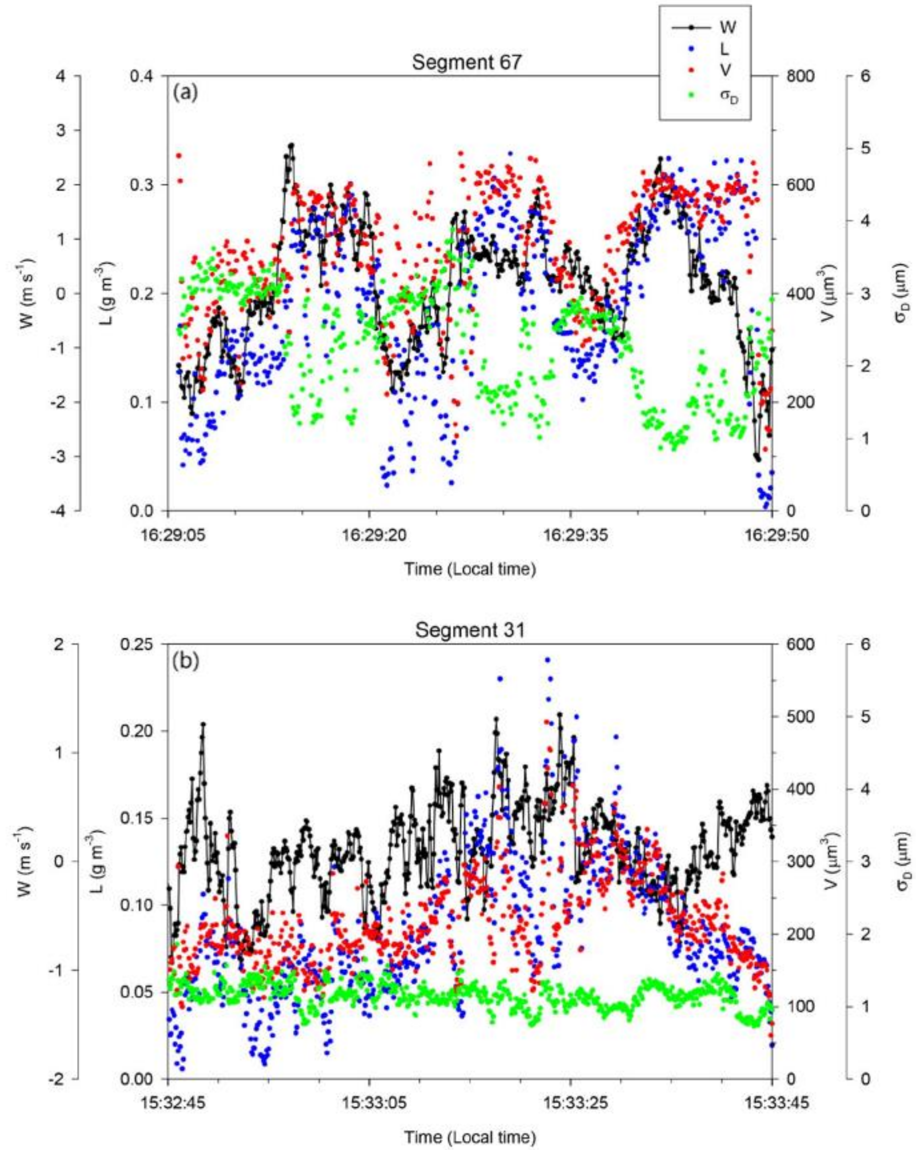

The environment conditions suggest more prevalent occurrence of homogeneous mixing.

Relationship between W and L suggests vertical circulation in most cases but not always.

- The relationship between θ_v and L does not support vertical circulation hypothesis.

- θ_v is higher for more diluted parcels, which means **that more buoyant parcels tend to descend.**

- This contradictory result is suspected to be related to the **limitation of humidity (T_d) measurement in clouds** during the RACORO campaign.

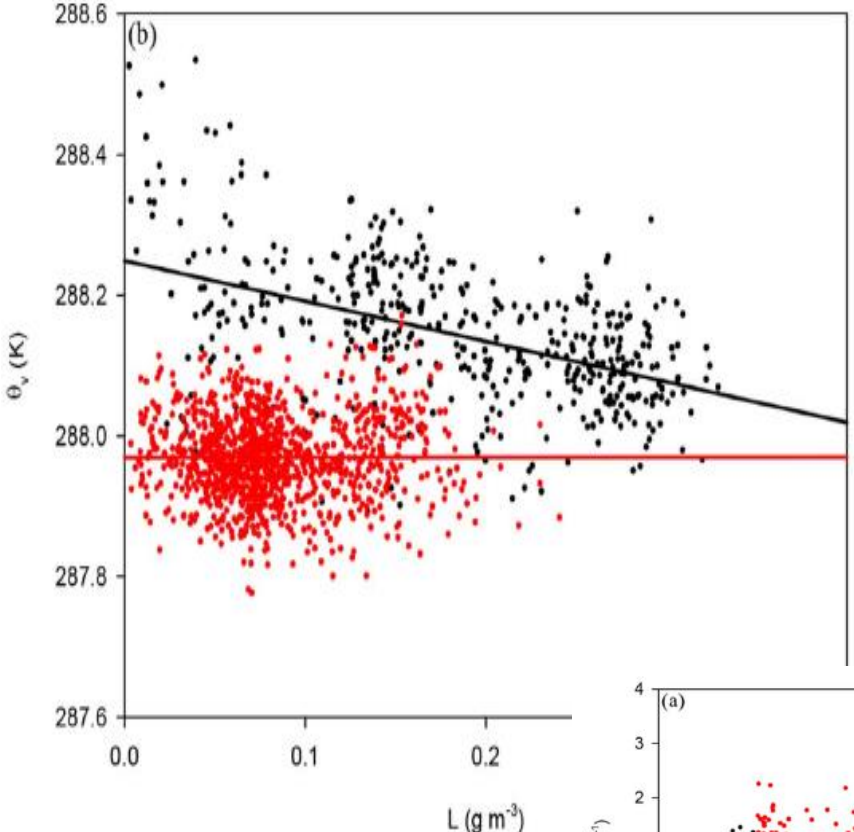

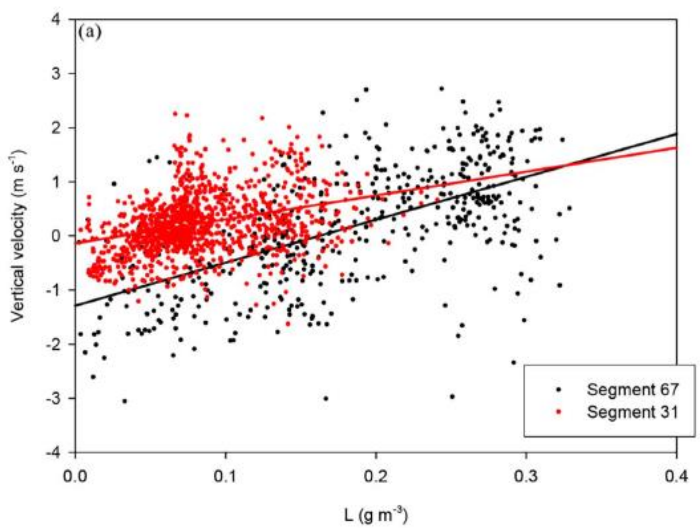

Aerosol and cloud experiments in the eastern north Atlantic (ACE-ENA)

1 June 2017 - 28 February 2018

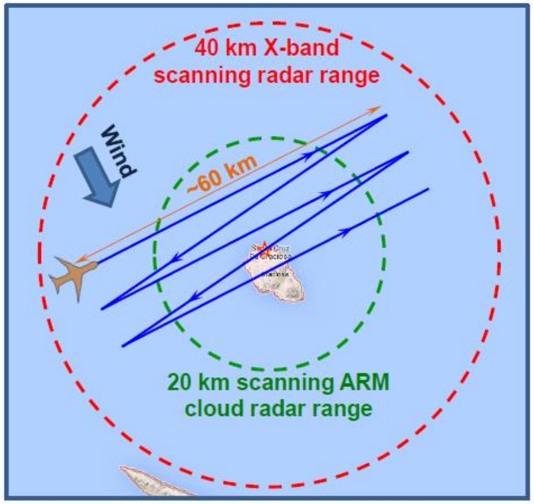

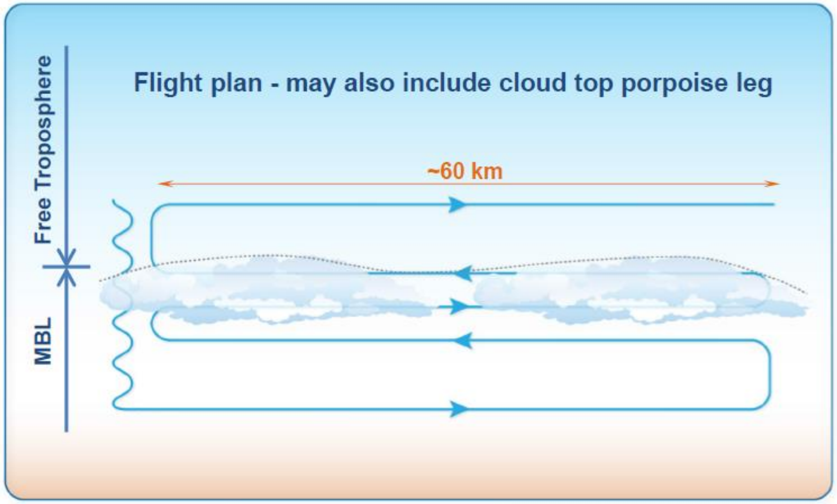

(Wang et al., 2016)

Example of cloud measurement

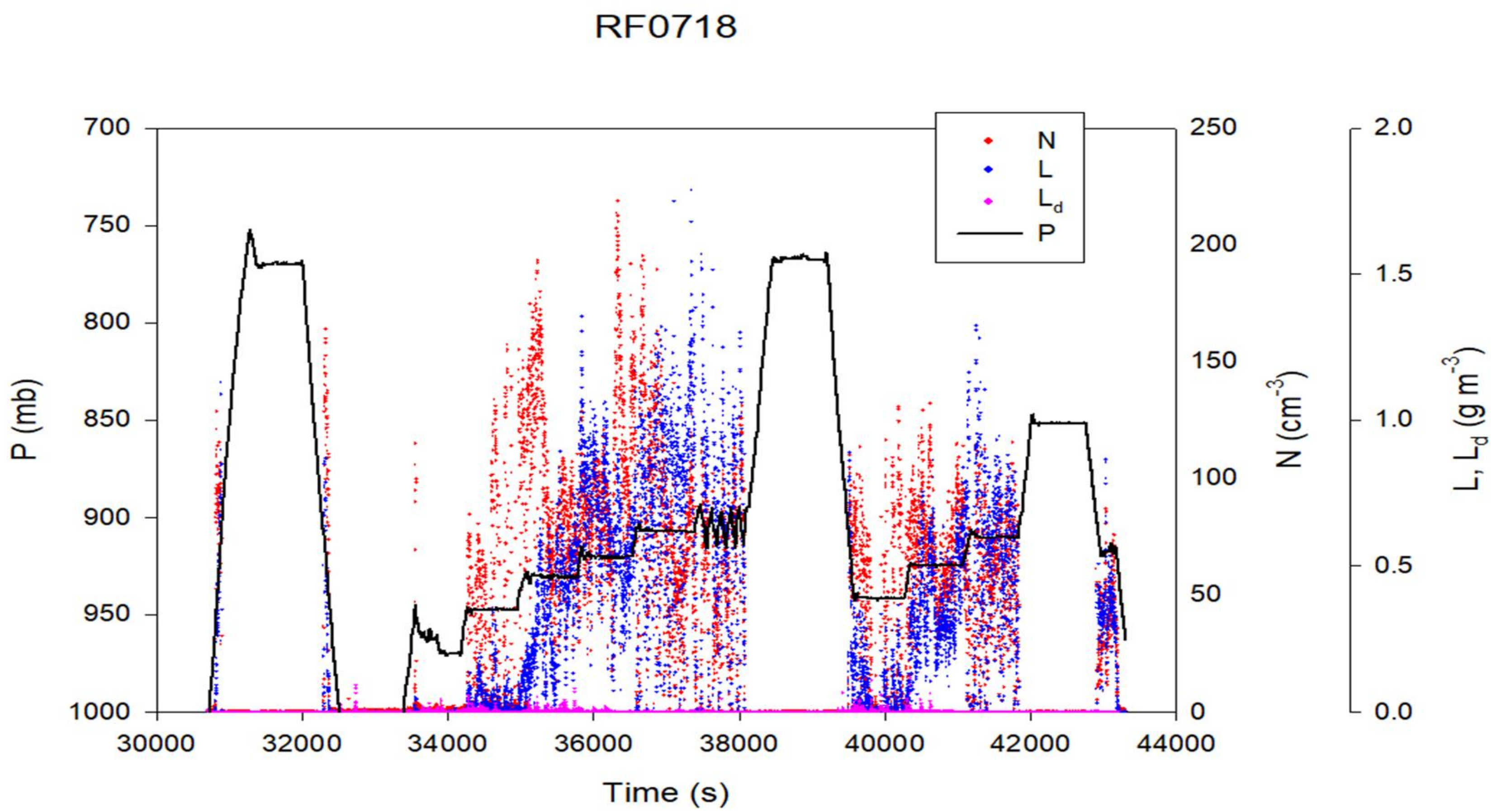

- During ACE-ENA campaign, **long horizontal penetrations at various altitudes** were made.

The relationships between cloud microphysical variables

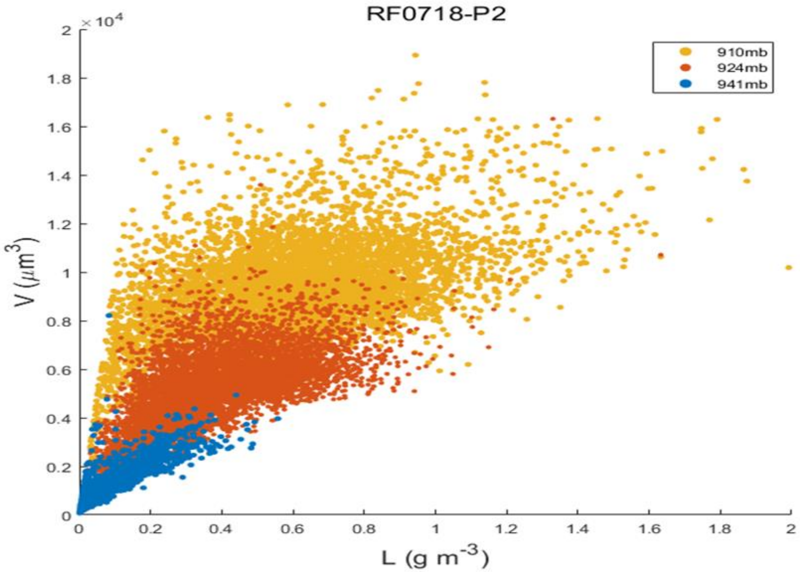

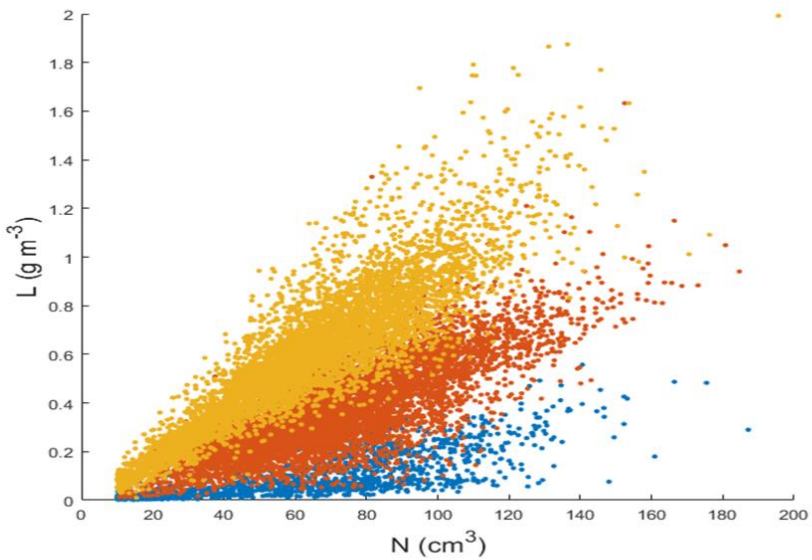

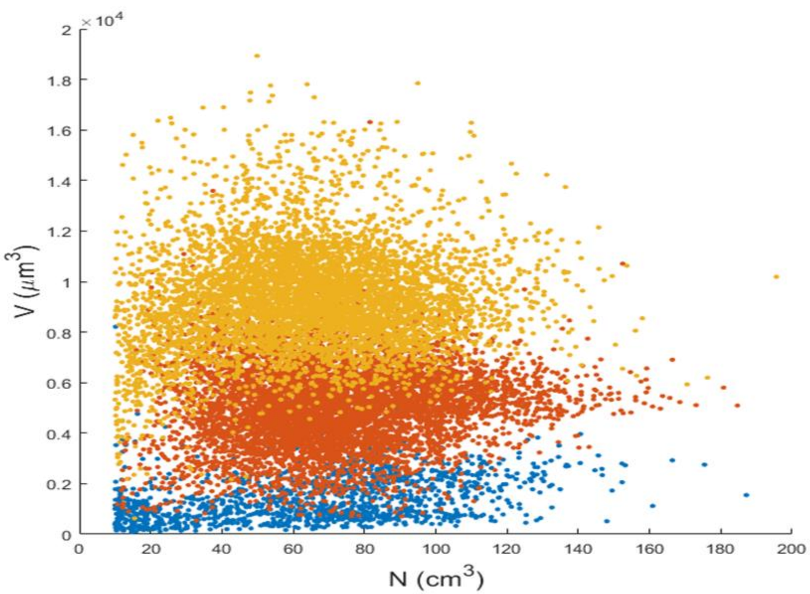

- Correlation between L and V exhibits **vertical variation**. As altitude goes down, it becomes **more positive**.
- L is positively correlated with N at all altitudes.
- Vague correlation between N and V.

Summary for examined penetrations

RF0712-P1	Γ_{N-L}	Γ_{N-V}	Γ_{L-V}
907 mb	0.73	-0.09	**0.56**
911 mb	0.27	-0.24	**0.83**
915 mb	0.44	0.09	**0.87**
918 mb	0.72	0.37	**0.83**
RF0712-P2			
921 mb	0.69	-0.21	**0.50**
925 mb	0.52	-0.24	**0.67**
928 mb	0.32	-0.26	**0.73**
932 mb	0.18	-0.19	**0.79**
936 mb	0.06	-0.17	**0.90**

RF0718-P1	Γ_{N-L}	Γ_{N-V}	Γ_{L-V}
906 mb	0.67	-0.48	**0.24**
920 mb	0.45	-0.46	**0.53**
929 mb	0.22	-0.38	**0.76**
947 mb	0.52	0.00	**0.72**
RF0718-P2			
910 mb	0.89	0.12	**0.51**
924 mb	0.79	0.11	**0.64**
941 mb	0.73	0.39	**0.81**

- All penetrations show the **same trends**: Γ_{L-V} is more positive as altitude goes down.

Mixing diagrams for a 20 s section at several sampling altitudes

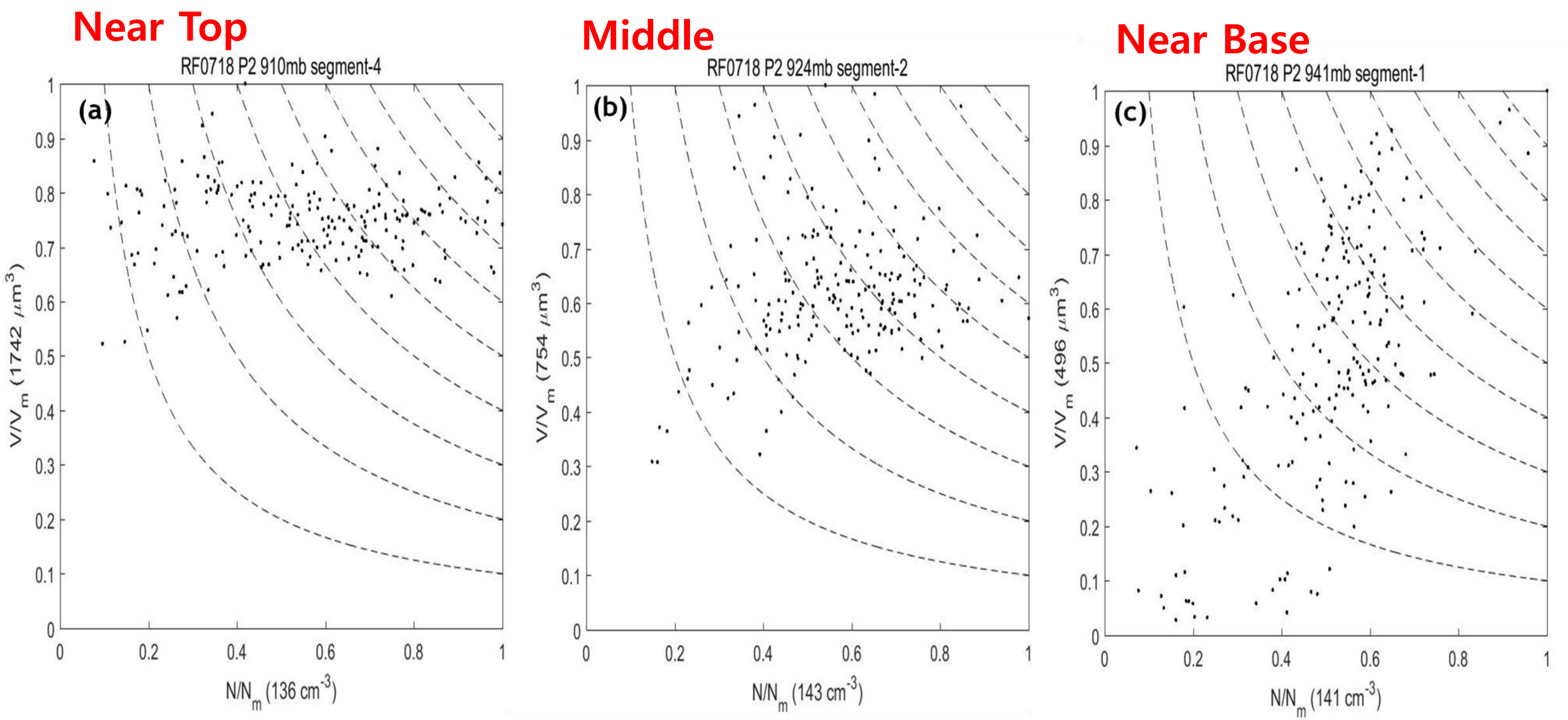

- Most cloud segments near cloud top show **IM trait**.
- Segments at middle and near cloud base suggest **HM trait**.

RF0718 P2

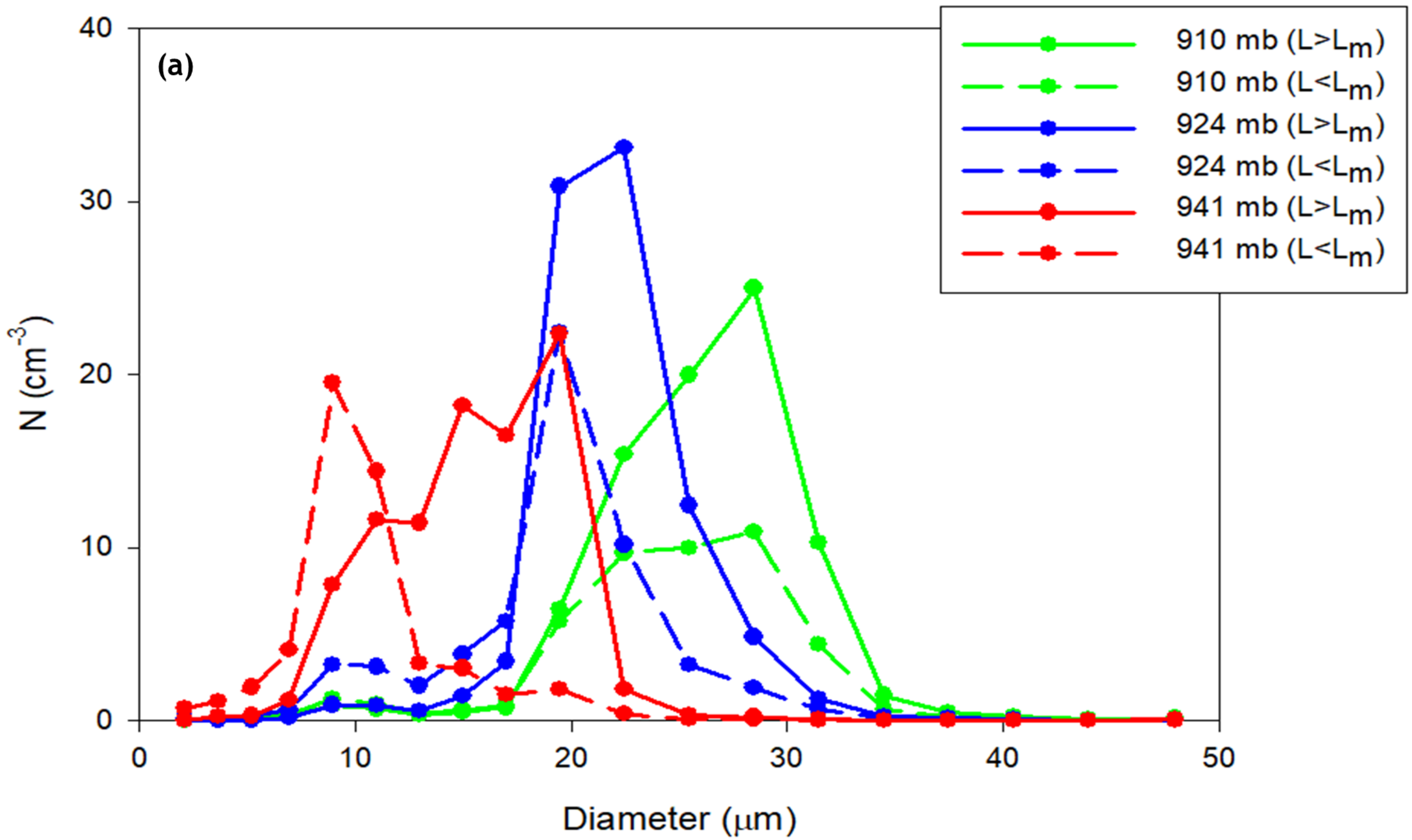

(a)
910 mb (L>Lm)
910 mb (L<Lm)
924 mb (L>Lm)
924 mb (L<Lm)
941 mb (L>Lm)
941 mb (L<Lm)
N (cm-3)
0
10
20
30
40
0
10
20
30
40
50
Diameter (μm)

RF0718-P1	$\Delta\theta_e$	$\kappa(L/C_p)\Delta q_t$
906 mb	-1.38	-1.00
920 mb	-1.43	-1.07
929 mb	-1.59	-1.04
947 mb	-5.09	-1.59
RF0718-P2		
910 mb	-1.01	-0.77
924 mb	-1.27	-0.85
941 mb	-3.13	-1.22

- The CTEI criterion is satisfied for RF0718 P1 and P2, implying that entrained and mixed parcels can be susceptible to downward movement through the cloud.

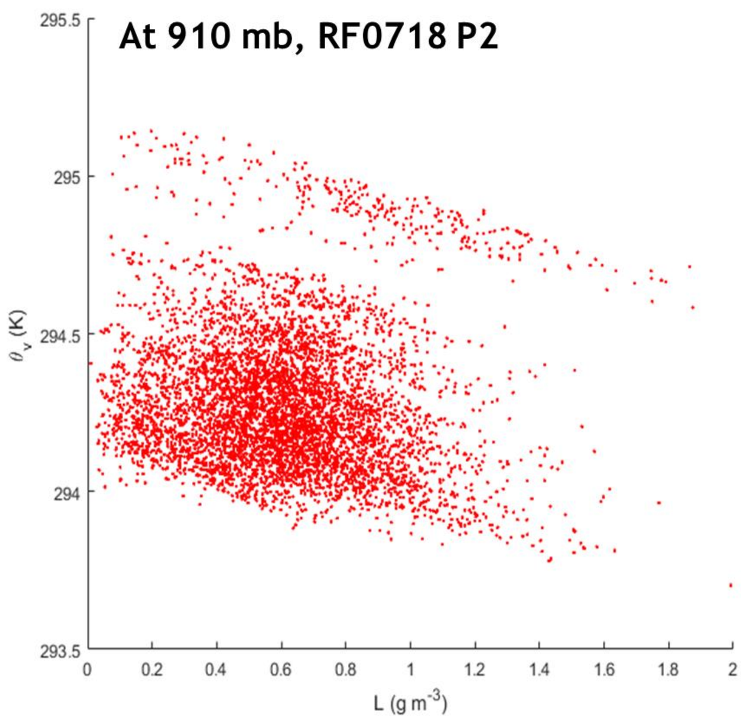

- Θ_v and L are negatively correlated, which is contradictory to the expectation of negative buoyancy of entrainment affected diluted parcels.

- Such contradictory results could be related to the measurement uncertainty of humidity in clouds.

Summary

- **Cloud microphysical relationships represented by mixing diagrams and linear correlation coefficients suggested HM for the maritime stratocumulus clouds (VOCALS, ACE-ENA, MASE (Wang et al., 2009)) and more so for continental stratocumulus clouds (RACORO).**

- **Moreover, evidence for IM or further growth after IM is not easily found. No super-adiabatic droplet growth caused by entrainment and mixing at least for the data presented here!**

- **Vertical circulation is speculated to be one of the crucial reasons why the HM traits is dominantly shown especially deeper down into the clouds.**

- **Then what?**
  - **"entrainment and mixing" is not a good potential mechanism that sets the stage for collision & coalescence.**
  - **Do the models capture these features? If not, what does it mean?**